Benzothiazole-Based Fluorophores of Donor−π-Acceptor−π-Donor Type Displaying High Two-Photon Absorption

Veronika Hrobáriková,[†,‡] Peter Hrobárik,*[,‡,§] Peter Gajdoš,[†] Ioannis Fitilis,[⊥] Mihalis Fakis,[⊥] Peter Persephonis,[⊥] and Pavol Zahradník[†]

[†]*Department of Organic Chemistry, Faculty of Natural Sciences, Comenius University, Mlynská dolina, SK-84215 Bratislava, Slovakia,* [‡]*Institut für Physikalische und Theoretische Chemie, Julius-Maximilians-Universität Würzburg, Am Hubland, DE-97074 Würzburg, Germany,* [§]*Institute of Inorganic Chemistry, Slovak Academy of Sciences, Dúbravská cesta 9, SK-84536 Bratislava, Slovakia, and* [⊥]*Department of Physics, University of Patras, GR-26504 Patras, Greece*

peter.hrobarik@savba.sk

Received February 25, 2010
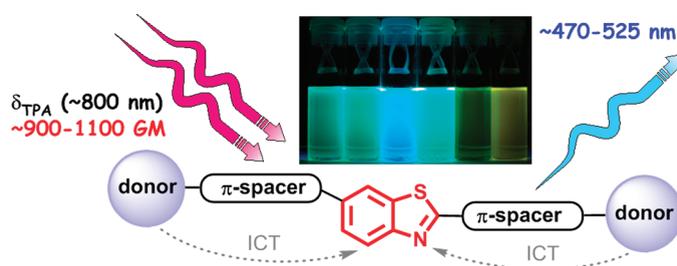
A series of novel heterocycle-based dyes with donor−π-bridge−acceptor−π-bridge−donor (D-π-A-π-D) structural motif, where benzothiazole serves as an electron-withdrawing core, have been designed and synthesized via palladium-catalyzed Sonogashira and Suzuki-type cross-coupling reactions. All the target chromophores show strong one-photon and two-photon excited emission. The maximum two-photon absorption (TPA) cross sections δ_{TPA} of the prepared derivatives bearing diphenylamino functionalities occur at wavelengths ranging from 760 to 800 nm and are as large as ∼900−1100 GM. One- and two-photon absorption characteristics of the title dyes have also been investigated by using density functional theory (DFT) and the structure−property relationships are discussed. The TPA cross sections calculated by means of quadratic response time-dependent DFT using the Coulomb-attenuated CAM-B3LYP functional support the experimentally observed trends within the series, as well as higher δ_{TPA} values of the title compounds compared to those of analogous fluorene or carbazole-derived dyes. In contrast, the traditional B3LYP functional was not successful in predicting the observed trend of TPA cross sections for systems with different central cores. In general, structural modification of the π-bridge composition by replacement of ethynylene (alkyne) with *E*-ethenylene (alkene) linkages and/or replacement of dialkylamino electron-donating edge substituents by diarylamino ones results in an increase of δ_{TPA} values. The combination of large TPA cross sections and high emission quantum yields makes the title benzothiazole-based dyes attractive for applications involving two-photon excited fluorescence (TPEF).

Introduction

The development of materials displaying high two-photon absorption (TPA)[1,2] has attracted great interest in the past decade due to a variety of potential applications in photonics and optoelectronics, such as three-dimensional optical data storage, fluorescence imaging, nonlinear optics, microfabrication, etc.[3] All these TPA-based applications benefit mainly from the following attributes of the two-photon absorption process: (a) the activation of high-energy photophysical properties by low-energy near-IR excitation (simultaneous absorption of two photons of half the excitation energy by a single molecule), resulting in larger material penetration compared to excitations by visible or UV light, and (b) quadratic

(1) Pawlicki, M.; Collins, H. A.; Denning, R. G.; Anderson, H. L. *Angew. Chem., Int. Ed.* **2009**, *48*, 3244–3266.

(2) Terenziani, F.; Katan, C.; Badaeva, E.; Tretiak, S.; Blanchard-Desce, M. *Adv. Mater.* **2008**, *20*, 4641–4678.

dependence of the two-photon absorption on the intensity of light, which allows for more control and higher spatial resolution. In view of biological applications, such as in vivo imaging, these advantages play an important role as they lead to a finer resolution and a better in-depth tissue penetration, combined with reduced cell damage. As a consequence, the two-photon microscopy experiences an increasing popularity.[4] Furthermore, the combination of the two-photon absorbers with efficient singlet oxygen generation offers great potential for further development of photodynamic cancer therapy (PDT) methods.[5] The two-photon absorption process is, however, statistically disfavored and hence the performance of classical one-photon fluorophores is usually not sufficient for a potential application, due to their low two-photon absorption cross sections (δ_{TPA}). To fully exploit the great potential of the TPA process, research focused on the design and synthesis of molecules exhibiting large δ_{TPA} is still ongoing.[6−9] Apart from the large TPA absorption, high two-photon excited fluorescence (TPEF) quantum yields, good photostability, appreciable solubility, and proper response wavelengths are also required to meet practical application needs in fields such as fluorescence microscopy or upconverted lasing.[10]

The strategy for the construction of molecules with large TPA cross sections has been studied both experimentally[11,12] and theoretically,[13,14] and a certain part of the structure−property relations has been explored. In particular, extended

π-conjugated systems symmetrically substituted with electron-donating (D) and/or electron-accepting (A) functionalities have been revealed as efficient TPA dyes. On the basis of this general setting, many factors play an important role in increasing δ_{TPA}, such as the efficiency of intramolecular charge transfer (ICT), the conjugation length, the molecular planarity, the dimensionality of the charge-transfer network, the vibronic coupling, and the donating and withdrawing abilities of the electron donor and acceptor.[15]

Although a number of efficient TPA chromophores are already available, many of them consist only from substituted conjugated aromatic rings, such as benzene or fluorene, and rely on the electronic properties of simple electron-donating and/or electron-withdrawing functionalities. Replacement of these aromatic systems with more easily delocalizable π-excessive or π-deficient heteroaromatics has been shown to result in an increased intramolecular charge transfer (ICT) as well as an enhanced two-photon absorption, while the chemical and photochemical stability of these systems has been preserved.[9,16] Moreover, modification of the structure by incorporation of heteroaromatics into π-conjugated systems allows for fine-tuning of the electronic and optical properties and often results in strong fluorescence emission, which is an essential prerequisite for certain TPA-based applications (vide supra).[17]

The employment of heterocycles, such as thiophene,[18,19] pyrrole,[19,20] or carbazole,[21,22] in the design of novel dyes with enhanced TPA has already been reported. Among various heterocycles, benzothiazole has attractive chemical and physical properties making it an appropriate building block in construction of chromophores for nonlinear optics.[23−25]

(3) Dvornikov, A. S.; Walker, E. P.; Rentzepis, P. M. *J. Phys. Chem. A* **2009**, *113*, 13633–13644. Tian, H.; Feng, Y. L. *J. Mater. Chem.* **2008**, *18*, 1617–1622. Barsu, C.; Cheaib, R.; Chambert, S.; Queneau, Y.; Maury, O.; Cottet, D.; Wege, H.; Douady, J.; Bretonniere, Y.; Andraud, C. *Org. Biomol. Chem.* **2010**, *8*, 142–150. Lin, T.-C.; Haung, Y.-J.; Chen, Y.-F.; Hu, C.-L. *Tetrahedron* **2010**, *66*, 1375–1882. LaFratta, C. N.; Fourkas, J. T.; Baldacchini, T.; Farrer, R. A. *Angew. Chem., Int. Ed.* **2007**, *46*, 6238–6258. Cumpston, B. H.; Ananthavel, S. P.; Barlow, S.; Dyer, D. L.; Ehrlich, J. E.; Erskine, L. L.; Heikal, A. A.; Kuebler, S. M.; Lee, I. Y.; McCord-Maughon, D.; Qin, J. Q.; Rockel, H.; Rumi, M.; Wu, X. L.; Marder, S. R.; Perry, J. W. *Nature* **1999**, *398*, 51–54.

(4) Zipfel, W. R.; Williams, R. M.; Webb, W. W. *Nat. Biotechnol.* **2003**, *21*, 1368–1376.

(5) Ogawa, K.; Kobuke, Y. *Org. Biomol. Chem.* **2009**, *7*, 2241–2246. Nielsen, C. B.; Arnbjerg, J.; Johnsen, M.; Jorgensen, M.; Ogilby, P. R. *J. Org. Chem.* **2009**, *74*, 9094–9104.

(6) Kim, H. M.; Lee, Y. O.; Lim, C. S.; Kim, J. S.; Cho, B. R. *J. Org. Chem.* **2008**, *73*, 5127–5130. Liu, Z. J.; Chen, T.; Liu, B.; Huang, Z. L.; Huang, T.; Li, S. Y.; Xu, Y. X.; Qin, J. G. *J. Mater. Chem.* **2007**, *17*, 4685–4689.

(7) Lartia, R.; Allain, C.; Bordeau, G.; Schmidt, F.; Fiorini-Debuisschert, C.; Charra, F.; Teulade-Fichou, M. P. *J. Org. Chem.* **2008**, *73*, 1732–1744.

(8) Bhaskar, A.; Ramakrishna, G.; Lu, Z. K.; Twieg, R.; Hales, J. M.; Hagan, D. J.; Van Stryland, E.; Goodson, T. *J. Am. Chem. Soc.* **2006**, *128*, 11840–11849.

(9) Shao, P.; Huang, B.; Chen, L. Q.; Liu, Z. J.; Qin, J. G.; Gong, H. M.; Ding, S.; Wang, Q. Q. *J. Mater. Chem.* **2005**, *15*, 4502–4506.

(10) Tian, Y.; Chen, C. Y.; Cheng, Y. J.; Young, A. C.; Tucker, N. M.; Jen, A. K. Y. *Adv. Funct. Mater.* **2007**, *17*, 1691–1697. Margineanu, A.; Hofkens, J.; Cotlet, M.; Habuchi, S.; Stefan, A.; Qu, J. Q.; Kohl, C.; Mullen, K.; Vercammen, J.; Engelborghs, Y.; Gensch, T.; De Schryver, F. C. *J. Phys. Chem. B* **2004**, *108*, 12242–12251. Porres, L.; Mongin, O.; Katan, C.; Charlot, M.; Pons, T.; Mertz, J.; Blanchard-Desce, M. *Org. Lett.* **2004**, *6*, 47–50.

(11) Kim, H. M.; Cho, B. R. *Chem. Commun.* **2009**, 153–164. Kim, H. M.; Seo, M. S.; Jeon, S. J.; Cho, B. R. *Chem. Commun.* **2009**, 7422–7424. Kamada, K.; Iwase, Y.; Sakai, K.; Kondo, K.; Ohta, K. *J. Phys. Chem. C* **2009**, *113*, 11469–11474.

(12) Fitilis, I.; Fakis, M.; Polyzos, I.; Giannetas, V.; Persephonis, P.; Vellis, P.; Mikroyannidis, J. *Chem. Phys. Lett.* **2007**, *447*, 300–304.

(13) Chakrabarti, S.; Ruud, K. *Phys. Chem. Chem. Phys.* **2009**, *11*, 2592–2596. Zein, S.; Delbecq, F.; Simon, D. *Phys. Chem. Chem. Phys.* **2009**, *11*, 694–702. Nguyen, K. A.; Day, P. N.; Pachter, R. *Theor. Chem. Acc.* **2008**, *120*, 167–175. Wang, C. K.; Macak, P.; Luo, Y.; Agren, H. *J. Chem. Phys.* **2001**, *114*, 9813–9820.

(14) Rudberg, E.; Salek, P.; Helgaker, T.; Agren, H. *J. Chem. Phys.* **2005**, *123*, 184108.

(15) Albota, M.; Beljonne, D.; Bredas, J. L.; Ehrlich, J. E.; Fu, J. Y.; Heikal, A. A.; Hess, S. E.; Kogej, T.; Levin, M. D.; Marder, S. R.; McCord-Maughon, D.; Perry, J. W.; Rockel, H.; Rumi, M.; Subramaniam, C.; Webb, W. W.; Wu, X. L.; Xu, C. *Science* **1998**, *281*, 1653–1656. Reinhardt, B. A.; Brott, L. L.; Clarson, S. J.; Dillard, A. G.; Bhatt, J. C.; Kannan, R.; Yuan, L. X.; He, G. S.; Prasad, P. N. *Chem. Mater.* **1998**, *10*, 1863–1874.

(16) Abbotto, A.; Beverina, L.; Bozio, R.; Facchetti, A.; Ferrante, C.; Pagani, G. A.; Pedron, D.; Signorini, R. *Org. Lett.* **2002**, *4*, 1495–1498. Zheng, S. J.; Beverina, L.; Barlow, S.; Zojer, E.; Fu, J.; Padilha, L. A.; Fink, C.; Kwon, O.; Yi, Y. P.; Shuai, Z. G.; Van Stryland, E. W.; Hagan, D. J.; Bredas, J. L.; Marder, S. R. *Chem. Commun.* **2007**, 1372–1374. Zou, L.; Liu, Z. J.; Yan, X. B.; Liu, Y.; Fu, Y.; Liu, J.; Huang, Z. L.; Chen, X. G.; Qin, J. G. *Eur. J. Org. Chem.* **2009**, 5587–5593.

(17) Kato, S.; Matsumoto, T.; Shigeiwa, M.; Gorohmaru, H.; Maeda, S.; Ishi-i, T.; Mataka, S. *Chem.—Eur. J.* **2006**, *12*, 2303–2317.

(18) Williams-Harry, M.; Bhaskar, A.; Rarnakrishna, G.; Goodson, T.; Imamura, M.; Mawatari, A.; Nakao, K.; Enozawa, H.; Nishinaga, T.; Iyoda, M. *J. Am. Chem. Soc.* **2008**, *130*, 3252–3253. Feng, Y. F.; Yan, Y. L.; Wang, S.; Zhu, W. H.; Qian, S. X.; Tian, H. *J. Mater. Chem.* **2006**, *16*, 3685–3692.

(19) Zheng, S. J.; Leclercq, A.; Fu, J.; Beverina, L.; Padilha, L. A.; Zojer, E.; Schmidt, K.; Barlow, S.; Luo, J. D.; Jiang, S. H.; Jen, A. K. Y.; Yi, Y. P.; Shuai, Z. G.; Van Stryland, E. W.; Hagan, D. J.; Bredas, J. L.; Marder, S. R. *Chem. Mater.* **2007**, *19*, 432–442.

(20) Beverina, L.; Crippa, M.; Landenna, M.; Ruffo, R.; Salice, P.; Silvestri, F.; Versari, S.; Villa, A.; Ciaffoni, L.; Collni, E.; Ferrante, C.; Bradamante, S.; Mari, C. M.; Bozio, R.; Pagani, G. A. *J. Am. Chem. Soc.* **2008**, *130*, 1894–1902. Jiang, Y. H.; Wang, Y. C.; Hua, J. L.; Qu, S. Y.; Qian, S. Q.; Tian, H. *J. Polym. Sci., Part A: Polym. Chem.* **2009**, *47*, 4400–4408.

(21) Yang, J. X.; Wang, C. X.; Li, L.; Lin, N.; Tao, X. T.; Tian, Y. P.; Zhao, X.; Jiang, M. H. *Chem. Phys.* **2009**, *358*, 39–44.

(22) Fitilis, I.; Fakis, M.; Polyzos, I.; Giannetas, V.; Persephonis, P.; Mikroyannidis, J. *J. Phys. Chem. A* **2008**, *112*, 4742–4748.

(23) Hrobarik, P.; Zahradnik, P.; Fabian, W. M. F. *Phys. Chem. Chem. Phys.* **2004**, *6*, 495–502. Zajac, M.; Hrobarik, P.; Magdolen, P.; Foltinova, P.; Zahradnik, P. *Tetrahedron* **2008**, *64*, 10605–10618.

(24) Hrobarik, P.; Sigmundova, I.; Zahradnik, P. *Synthesis* **2005**, 600–604.

(25) Batista, R. M. F.; Costa, S. P. G.; Malheiro, E. L.; Belsley, M.; Raposo, M. M. M. *Tetrahedron* **2007**, *63*, 4258–4265. Costa, S. P. G.; Batista, R. M. F.; Cardoso, P.; Belsley, M.; Raposo, M. M. M. *Eur. J. Org. Chem.* **2006**, 3938–3946.
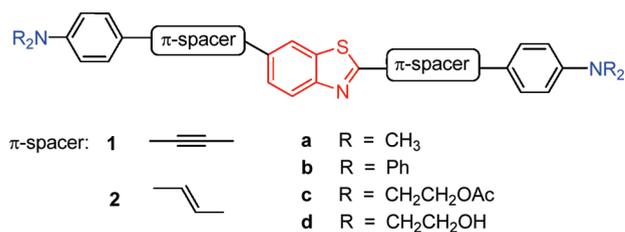
FIGURE 1. Schematic structures of the novel benzothiazole-based fluorophores of D-π-A-π-D type.

FIGURE 2. Structural analogues of **2b** containing fluorene (**3**) or carbazole (**4**) core.

Recently, several two-photon absorbing dyes containing benzothiazole as an electron-withdrawing edge substituent have been synthesized, and fairly good values of TPA cross sections have been measured for them.[7,9,26] However, to the best of our knowledge, there is no report on TPA dyes utilizing benzothiazole as the electron-withdrawing central core. Thus, to fully explore the potential of the benzothiazole unit, an extension to derivatives of this novel class is highly desirable. Particularly interesting would be structures with the D-π-A-π-D constitution (cf. Figure 1), where a 2-fold intramolecular charge transfer between the end and the center of the molecule could take place. Due to the unsymmetrical nature of the benzothiazole unit, these compounds could be viewed as quasi-quadrupolar systems with nonzero dipolar moments and partially preserved push–pull character. The question is also to what extent the redistribution of charge upon photoexcitation is asymmetrical, since there is no center of symmetry in these systems.

Herein, we report the synthesis and characterization, the linear optical absorption and fluorescence, as well as the TPA properties of six novel benzothiazole-derived dyes possessing a general D-π-A-π-D-type structure. All the studied molecules contain electron-donating dialkylamino or diphenylamino functionalities conjugated through planar phenylene-ethynylene (**1**) or phenylene-ethenylene (**2**) spacers to the electron-withdrawing benzothiazole core. To increase the solubility of the title dyes in more polar solvents, two derivatives containing hydroxy or acetyloxy groups at the donor periphery were also prepared. One-photon and two-photon absorption properties of target compounds are investigated both experimentally and theoretically by means of a TPEF technique with femtosecond pulsed excitation and density functional theory calculations, respectively. Experimentally measured and calculated δ_{TPA} values are discussed and confronted with those of analogous D-π-D and D-π-D-π-D systems, where the benzothiazole core is replaced by a fluorene (**3**)[12] or a carbazole (**4**)[12] ring (Figure 2).

Results and Discussion

I. Synthesis. The synthesis of the target compounds **1a–d**, with ethynylene spacers connecting the benzothiazole and the phenyl functionalities, was achieved by using a double Sonogashira-type cross-coupling reaction[27] between

2,6-diiodo-1,3-benzothiazole (**5**) and terminal phenylacetylenes **7a–d**, catalyzed by [Pd(PPh$_3$)$_2$Cl$_2$] and CuI (Scheme 1). Products **1a–d** were obtained in good yields ranging from 57% to 80%. Employment of 2,6-dibromobenzothiazole (**6**) under the same reaction conditions led predominantly to the product of monocoupling (in the C-2 position of the benzothiazole), even if a large excess of phenylacetylene (up to the 10 equiv) was used.

In contrast to the ease of the Sonogashira-type reaction, a double Suzuki-type cross-coupling reaction[28] of **5** with boronic esters, prepared "in situ" via addition of catecholborane to the triple bond of phenylacetylenes **7a,b**, afforded the expected products **2a,b** in only low yields (ca. 10%) and with poor reproducibility. Therefore, an alternative synthetic strategy for the formation of target compounds **2** was proposed. This included a mono-Suzuki cross-coupling reaction between 6-iodo-2-methylbenzothiazole (**8**) and the corresponding boronic esters derived from the phenylacetylenes **7a,b**, followed by an aldol-type condensation of the resulting 6-substituted-2-methylbenzothiazoles **9a,b** with suitable benzaldehydes (**10a,b**), catalyzed by KOH in DMSO (Scheme 2).

The donor-substituted phenylacetylenes **7a,c,d** were prepared via Sonogashira-type alkynylation of 4-iodo-*N,N*-dialkylanilines **11a,c,d** with trimethylsilylacetylene[29] or propargylalcohol.[30] The desired terminal alkynes were obtained by a subsequent removal of the TMS moiety with tetrabutylammonium fluoride (TBAF) or by a subsequent oxidation of the primary alcohol **12** followed by deformylation of the intermediated aldehyde **13** with MnO$_2$ and KOH, in overall good yields (Scheme 3). The same protocol is applicable also for the preparation of the *N,N*-diphenylamino derivative **7b**, as was shown in ref 31. However, the 4-iodo-*N,N*-diphenylaminobenzene (**11b**) is not directly accessible via iodination of triphenylamine because of its high reactivity (reaction ultimately results in a mixture of overhalogenated compounds).[32] Instead, a palladium-catalyzed Buchwald–Hartwig reaction

(26) Cao, D. X.; Fang, Q.; Wang, D.; Liu, Z. Q.; Xue, G.; Xu, G. B.; Yu, W. T. *Eur. J. Org. Chem.* **2003**, 3628–3636. Mikhailov, I. A.; Bondar, M. V.; Belfield, K. D.; Masunov, A. E. *J. Phys. Chem. C* **2009**, *113*, 20719–20724. Rogers, J. E.; Slagle, J. E.; McLean, D. G.; Sutherland, R. L.; Brant, M. C.; Heinrichs, J.; Jakubiak, R.; Kannan, R.; Tan, L. S.; Fleitz, P. A. *J. Phys. Chem. A* **2007**, *111*, 1899–1906.

(27) Sonogashira, K.; Tohda, Y.; Hagihara, N. *Tetrahedron Lett.* **1975**, 4467–4470. Chinchilla, R.; Najera, C. *Chem. Rev.* **2007**, *107*, 874–922. Doucet, H.; Hierso, J. C. *Angew. Chem., Int. Ed.* **2007**, *46*, 834–871.

(28) Miyaura, N.; Suzuki, A. *Chem. Rev.* **1995**, *95*, 2457–2483. Suzuki, A. *J. Organomet. Chem.* **1999**, *576*, 147–168. McGlacken, G. P.; Fairlamb, I. J. S. *Eur. J. Org. Chem.* **2009**, 4011–4029.

(29) Jian, H. H.; Tour, J. M. *J. Org. Chem.* **2003**, *68*, 5091–5103. Zhang, X. J.; Ren, X. S.; Xu, Q. H.; Loh, K. P.; Chen, Z. K. *Org. Lett.* **2009**, *11*, 1257–1260.

(30) Godt, A. *J. Org. Chem.* **1997**, *62*, 7471–7474.

(31) McIlroy, S. P.; Clo, E.; Nikolajsen, L.; Frederiksen, P. K.; Nielsen, C. B.; Mikkelsen, K. V.; Gothelf, K. V.; Ogilby, P. R. *J. Org. Chem.* **2005**, *70*, 1134–1146.

(32) Allain, C.; Schmidt, F.; Lartia, R.; Bordeau, G.; Fiorini-Debuisschert, C.; Charra, F.; Tauc, P.; Teulade-Fichou, M. P. *ChemBioChem* **2007**, *8*, 424–433.

SCHEME 1.   Preparation of Target Compounds 1a−d via Sonogashira Cross-Coupling Reaction

1a R= CH₃ (80%) **1c** R= CH₂CH₂OAc (57%)
1b R= Ph (74%) **1d** R= CH₂CH₂OH (66%)
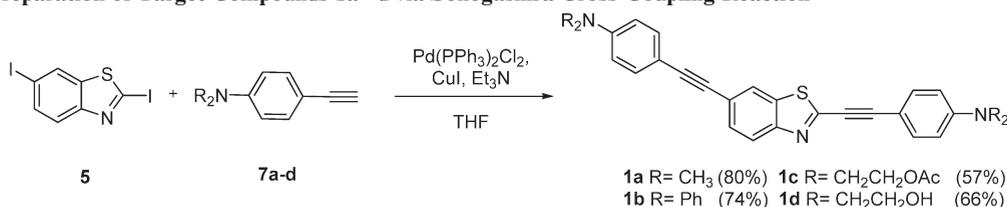
SCHEME 2.   Preparation of Target Compounds 2a,b via Suzuki Cross-Coupling Reaction and Condensation

9a R= CH₃ (78%)
9b R= Ph (90%)

10a-b
DMSO, KOH (aq.)

2a R= CH₃ (65%)
2b R= Ph   (55%)
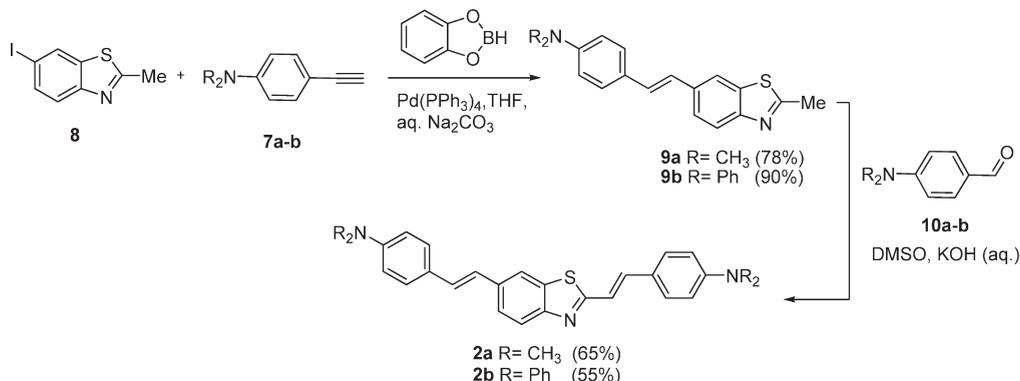
SCHEME 3.   Synthesis of the Phenylacetylenes 7a−d

7a (75%)
7c (70%)
7d (74%)

11a R= CH₃
11c R= CH₂CH₂OAc
11d R= CH₂CH₂OH

12a (78%)
12c (84%)

13c (67%)

7a (72%)
7c (90%)

7b (45%)

14 (68%)

10b

7b (60%)
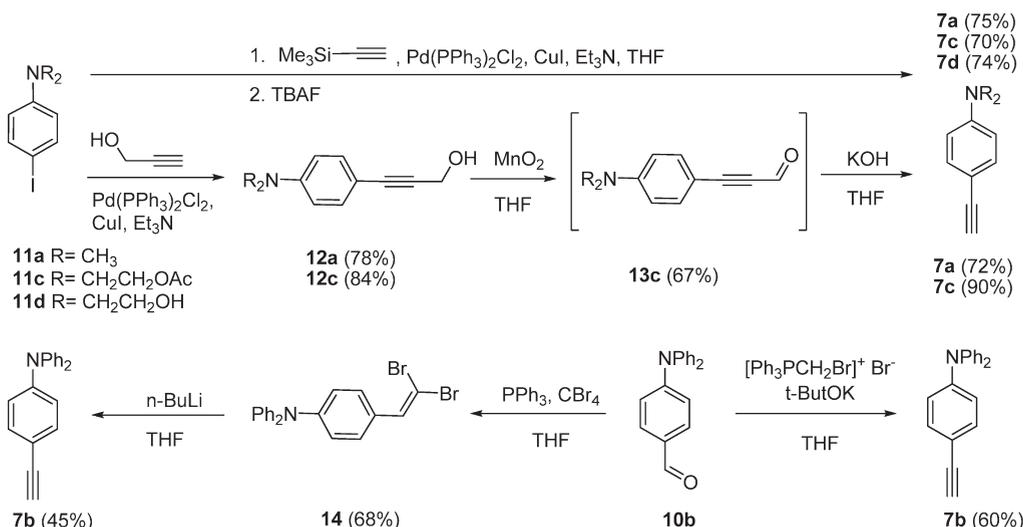
between diphenylamine and 1,4-dihalobenzene is often employed.[33] Aware of this, alternative routes to prepare **7b** were proposed. The readily available *N*,*N*-diphenylaminobenzaldehyde (**10b**) was transformed to **7b** by using a Wittig-type condensation[34] with (bromomethyl)triphenylphosphonium bromide in the presence of excess potassium *tert*-butoxide in 60% yield. Similarly, the aldehyde **10b** undergoes a Corey−Fuchs transformation[35] with CBr₄/PPh₃ and a subsequent dehalogenation of the intermediated β,β-dibromo-4-diphenyl-

aminostyrene (**14**) with *n*-BuLi to give **7b** in overall 31% yield (Scheme 3). Thus, the former method was found to be more efficient. At this point, it is worthwhile to mention that the prepared phenylacetylenes **7a−d** could serve as convenient precursors for the synthesis of various optoelectronic materials.

2,6-Dibromobenzothiazole (**6**) was prepared in the following sequence: 4-Bromoaniline (**15b**) was reacted with thiocyanogen,[36] generated from ammonium thiocyanate and molecular bromine in acetic acid, to give 2-amino-6-benzothiazole (**16b**) in 75% yield. **16b** was then smoothly transformed to 2,6-dibromobenzothiazole (**6**) by means of a

(33) Wang, C. S.; Palsson, L. O.; Batsanov, A. S.; Bryce, M. R. *J. Am. Chem. Soc.* **2006**, *128*, 3789–3799.
(34) Matsumoto, M.; Kuroda, K. *Tetrahedron Lett.* **1980**, *21*, 4021–4024.
(35) Corey, E. J.; Fuchs, P. L. *Tetrahedron Lett.* **1972**, 3769–3772. Hwang, G. T.; Son, H. S.; Ku, J. K.; Kim, B. H. *J. Am. Chem. Soc.* **2003**, *125*, 11241–11248. Khan, Z. A.; Wirth, T. *Org. Lett.* **2009**, *11*, 229–231.

(36) Jordan, A. D.; Luo, C.; Reitz, A. B. *J. Org. Chem.* **2003**, *68*, 8693–8696.

SCHEME 4. Synthesis of the Benzothiazole Compounds 5, 6, and 8
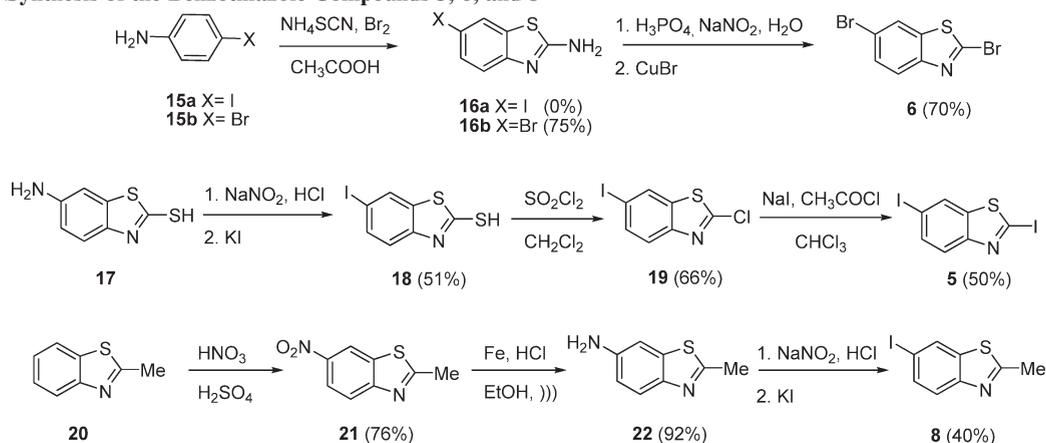
Sandmeyer reaction with copper(I) bromide (Scheme 4). Attempts to prepare the hitherto unknown 2,6-diiodobenzothiazole (**5**) in a similar way failed. Hence alternative approaches were investigated, such as (a) a 2-fold diazotation of 2,6-diaminobenzothiazole[37] followed by a quenching of corresponding diazonium salt with aqueous solution of KI or (b) introducing iodine into the C-6 position of commercially available 6-aminobenzothiazole-2-thiol (**17**) and subsequent replacement of the thiol group with halogen. After extensive experimentation, the latter method was revealed to be particularly efficient. Substitution of the 2-thiol group in **18** with chlorine was successfully accomplished by reaction with SO_2Cl_2.[38] The obtained 2-chloro-6-iodobenzothiazole (**19**) was then converted to 2,6-diiodobenzothiazole (**5**) by treatment with sodium iodide in the presence of acetyl chloride in good yield (50%) (cf. Scheme 4). The latter reagent catalyzes the reaction by quaternization of the heterocyclic nitrogen with the acetyl group, which allows smooth nucleophilic substitution of chlorine by iodine.[39] Extension of the reaction time and/or elevation of the reaction temperature led to removal of the iodine from the C-2 position of benzothiazole. The starting 6-iodo-2-methylbenzothiazole (**8**), employed in a Suzuki cross-coupling reaction, was prepared by nitration of 2-methylbenzothiazole (**20**), subsequent sonochemical reduction of **21**, and replacement of the amino group in **22** with iodine via diazonium salt (Scheme 4).

II. One-Photon Absorption and Emission Properties. One-photon absorption and emission spectra of the benzothiazole derived dyes **1a,b** and **2a,b** in THF solutions are shown in Figure 3. The corresponding absorption λ_{abs} and emission λ_f maxima, as well as the fluorescence quantum yields Φ_f of all benzothiazole-containing systems under study, are presented in Table 1. All molecules absorb light in the violet spectral region (ca. 400−430 nm) and emit light in the blue-green region with peaks ranging from 472 to 525 nm, whereby the fluorescence Stokes shifts vary between 76 and 100 nm. The maximum molar extinction coefficient ε_{max}, corresponding to the amplitude of the absorption peak, remains essentially unchanged across the series.

(37) Cao, X.; You, Q. D.; Li, Z. Y.; Liu, X. R.; Xu, D.; Guo, Q. L.; Shang, J.; Chern, J. W.; Chen, M. L. *Bioorg. Med. Chem. Lett.* **2008**, *18*, 6206–6209.
(38) Zhu, L.; Zhang, M. B.; Dai, M. *J. Heterocycl. Chem.* **2005**, *42*, 727–730.
(39) Corcoran, R. C.; Bang, S. H. *Tetrahedron Lett.* **1990**, *31*, 6757–6758.
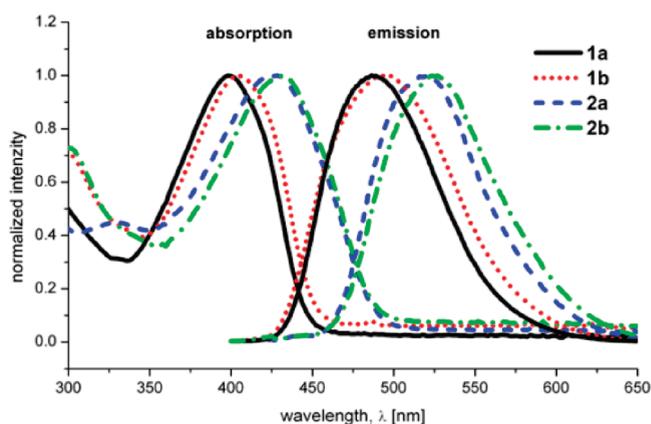
FIGURE 3. Normalized one-photon absorption and emission spectra of **1a,b** and **2a,b** in THF.

The fluorescence spectra exhibit a single peak, which indicates that the emission occurs from the lowest excited state with the largest oscillator strength. The quantum yields lie in the range of 0.14 to 0.57 and are, in general, larger for π-systems containing two triple bonds **1**. The replacement of a dialkylamino functionality with a diarylamino group results in slightly lower excitation energies E_{max}. A more pronounced red-shift is, however, achieved by a substitution of the ethynylene with an ethenylene spacer (ca. 0.2 eV).

It is noteworthy that these trends within the series are consistent with data calculated for **1a,b** and **2a,b** at the DFT level of theory as reported in Table 2 (see the Computational Method section for more details). The fairly good agreement between the theoretical and the experimental results for vertical excitation energies (E_{max}) encouraged us to analyze the absorption and emission spectral characteristics of **1** and **2** in more detail. The squares of the configuration interaction coefficients (configuration weights) obtained by time-dependent DFT (cf. Table 2) reveal that the two lowest energy excitations are associated with intramolecular charge transfer (ICT) and correspond predominantly to the transitions from valence HOMO (highest occupied molecular orbital) and HOMO−1 orbitals to the LUMO (lowest unoccupied molecular orbital) and LUMO+1 orbitals. The appearance of the relevant π-type orbitals for **2b** is demonstrated in Figure 4. Both HOMO and HOMO−1 are mainly constrained

TABLE 1.   Experimentally Determined One- and Two-Photon Optical Properties[a]

compd	λ_{abs} [nm] (E_{max} [eV])	log ε_{max}	λ_f [nm] (E_{em} [eV])	Φ_f	Stokes shift [nm]	δ_{TPA} [GM][b] (λ_{TPA} [nm])
1a	398 (3.12)	4.71	494 (2.51)	0.45	96	286 (750)
1b	404 (3.07)	4.70	488 (2.54)	0.57	84	902 (760)
1c	396 (3.13)	4.75	472 (2.63)	0.57	76	308 (750)
1d	406 (3.05)	4.75	492 (2.52)	0.48	86	807 (750)
2a	425 (2.92)	4.84	525 (2.36)	0.14	100	602 (750)
2b	429 (2.89)	4.83	519 (2.39)	0.43	90	1110 (800)
3	378 (3.28)		471 (2.63)	0.65	93	525 (750)
4	365 (3.40)		483 (2.57)	0.21	118	< 100 (750)

[a]All measurements were done in THF. [b]TPA cross sections are given in GM (1 GM = 1.10^{-50} cm$^4 \cdot$photon^{-1}); the position of maxima in the measurement range 750–840 nm is given in parentheses

TABLE 2.   Calculated Excitation Properties and Estimated TPA Cross Sections[a,b]

system	n	E_{max} [eV]	μ_{0n} [D]	$\Delta\mu_{0n}$ [D]	character of transitions (dominant contributions)		μ_{12} [D]	E_{em} [eV]	δ_{TPA}[c] [GM]
1a	1	3.39 (3.23)	14.21 (15.17)	2.50 (0.78)	78%	HOMO→LUMO	12.61 (14.12)	3.02 (2.85)	25 (8)
					10%	HOMO−1→LUMO			
	2	4.10 (3.88)	1.25 (1.79)	2.76 (3.97)	63%	HOMO−1→LUMO			1353 (1869)
					18%	HOMO→LUMO+1			
1b	1	3.27 (3.16)	15.70 (16.21)	0.95 (2.21)	63%	HOMO→LUMO	13.62 (14.97)	2.82 (2.65)	11 (40)
					14%	HOMO−1→LUMO			
	2	3.82 (3.66)	1.95 (2.67)	2.71 (3.85)	50%	HOMO−1→LUMO			1624 (2009)
					27%	HOMO→LUMO+1			
2a	1	3.22 (3.06)	14.66 (15.54)	2.35 (0.71)	79%	HOMO→LUMO	11.54 (13.27)	2.94 (2.81)	24 (9)
					9%	HOMO−1→LUMO			
	2	3.95 (3.72)	1.61 (2.15)	2.52 (3.04)	63%	HOMO−1→LUMO			1297 (1840)
					25%	HOMO→LUMO+1			
2b	1	3.12 (3.02)	15.98 (16.45)	0.80 (1.56)	70%	HOMO→LUMO	12.86 (14.60)	2.75 (2.64)	10 (18)
					12%	HOMO−1→LUMO			
	2	3.70 (3.56)	2.07 (2.71)	2.59 (2.74)	54%	HOMO−1→LUMO			1614 (2141)
					30%	HOMO→LUMO+1			
3	1	3.19 (3.13)	16.22 (16.67)	0.96 (1.01)	77%	HOMO→LUMO	8.75 (9.44)	2.94 (2.85)	13 (19)
					13%	HOMO−1→LUMO+1			
	2	3.72 (3.60)	3.41 (3.84)	2.52 (2.19)	52%	HOMO−1→LUMO			710 (818)
					35%	HOMO→LUMO+1			
4	1	3.20 (3.14)	16.08 (16.55)	0.90 (1.00)	77%	HOMO→LUMO	7.53 (8.31)	2.80 (2.71)	11 (17)
					13%	HOMO−1→LUMO+1			
	2	3.73 (3.61)	3.52 (4.01)	2.99 (2.45)	50%	HOMO−1→LUMO			517 (624)
					35%	HOMO→LUMO+1			

[a]Calculated at the CAM-B3LYP/6-31G(d) level of theory in vacuo (see Computational Details). [b]Data calculated with the PCM solvation model are given in parentheses. [c]Estimated from the three-state model.

to the donor part, whereas the LUMO and LUMO+1 have their largest atomic orbital (AO) coefficients at the atoms of the electron-withdrawing benzothiazole and adjacent ethynylene or ethenylene spacers. However, other carbon atoms in a π-conjugated bridge also contribute to all of these orbitals, leading to their extensive overlap, and thus to relatively large transition dipole moments. This is particularly evident in the case of the μ_{01} values (cf. Table 2).

At this point, it has to be noted that although both the B3LYP and the CAM-B3LYP functionals predict the same trends in the excitation energies with respect to the structural changes within the series, they provide a somewhat different picture regarding the character of the electronic transitions.

On the basis of the configuration weights and natural charge analysis of the ground state and the first two excited states at the B3LYP level (cf. Tables S1 and S3, Supporting Information), the lowest and strongest absorption band in the visible region ($S_0 \rightarrow S_1$) is almost exclusively composed of the HOMO−LUMO electronic excitation, and corresponds to the charge transfer from the electron-donating edge linked at the C-6 position of benzothiazole to the central electron-withdrawing core. The simultaneous charge transfer from both donor functionalities to the benzothiazole core ($S_0 \rightarrow S_2$) is

energetically disfavored and exhibits a notably smaller transition moment μ_{02}. The electronic transitions obtained by using the CAM-B3LYP functional have, however, considerably mixed characters as illustrated by the configuration weights of the principal configurations. This is reflected in a much smaller dipolar character of the first excited state (substantially lower values of $\Delta\mu_{01}$) and smaller excited-to-excited transition dipole moments μ_{12} compared to those calculated by the B3LYP method (cf. Table 2 and Table S1 in the Supporting Information). Since the CAM-B3LYP results are more reliable in this study (vide infra), the molecules under consideration should be viewed as quasi-quadrupolar structures with little dipolar character. Unfortunately, this feature prevents them from being applied simultaneously in TPEF as well as in second harmonic (SHG) imaging microscopy.[40]

Since a proper account of the solvent effect is very important for a direct comparison between experiment and calculations, we carried out TD-DFT calculations with the

(40) Barsu, C.; Fortrie, R.; Nowika, K.; Baldeck, P. L.; Vial, J. C.; Barsella, A.; Fort, A.; Hissler, M.; Bretonniere, Y.; Maury, O.; Andraud, C. *Chem. Commun.* **2006**, 4744–4746.
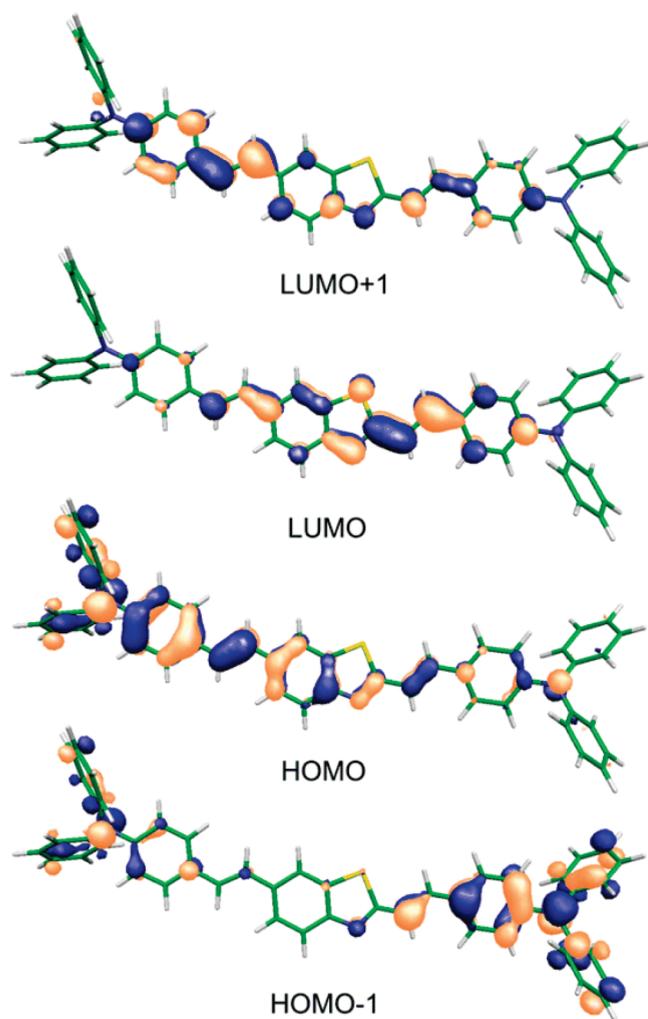
FIGURE 4. Two highest occupied and two lowest unoccupied molecular orbitals in **2b**.

FIGURE 5. Two-photon absorption cross sections δ_{TPA} (in GM units) of **1a−d** and **2a,b** in THF.

inclusion of bulk solvent effects via a polarizable continuum model (PCM) as well (cf. Table 2).[41,42] Comparing the results computed in vacuo and using the PCM model, it is evident that the effect of the solvent shifts both $E_{max,1}$ and $E_{max,2}$ to lower energies (by ca. 0.1−0.2 eV). In general, this effect is more pronounced for derivatives with a dimethylamino group (**1a**, **2a**), where the nitrogen lone pair is more accessible than in the case of a bulky diphenylamino moiety. The positive solvatochromism is consistent with the ICT character of both excited states and can be explained by their higher stabilization compared to the ground state by the polar THF solvent. Calculations with the PCM solvation model resulted also in slightly higher values of μ_{01} and μ_{12}. Overall, the B3LYP method underestimates the vertical excitation energies of the first excited state by ca. 0.3 eV with respect to the experimental values, while the CAM-B3LYP results are overestimated by 0.1 eV, showing a better performance of the latter method. The experimentally obtained

(41) Luo, Y.; Norman, P.; Macak, P.; Agren, H. *J. Phys. Chem. A* **2000**, *104*, 4718–4722. Nguyen, K. A.; Day, P. N.; Pachter, R. *J. Chem. Phys.* **2007**, *126*, 094303.
(42) Frediani, L.; Rinkevicius, Z.; Agren, H. *J. Chem. Phys.* **2005**, *122*, 244104.

Stokes shifts lie in the range of 0.5−0.6 eV, while the calculated ones vary from 0.3 to 0.5 eV.

The linear optical properties of compounds **1c** and **1d** were also experimentally examined in more polar solvents such as acetone, DMF, DMSO, and a mixture of DMSO and water (w/w = 1:1). The absorption spectra in these solvents were similar to those measured in THF and only a moderate red-shift of 0.1 eV (acetone) up to 0.2 eV (DMSO/H_2O) was observed. A more pronounced bathochromic shift with increasing solvent polarity was, however, noticed in the fluorescence emission spectra, confirming an ICT state formation.

III. Two-Photon Absorption. The two-photon cross sections were obtained by the two-photon induced fluorescence technique, using femtosecond laser pulses (see the Experimental Section). In all cases, the output intensity of two-photon excited fluorescence was linearly dependent on the square of the input laser intensity, thereby confirming the TPA process. The corresponding two-photon excitation spectra of compounds **1** and **2** in THF for excitation wavelengths ranging from 750 to 840 nm are shown in Figure 5.

The maximum values of the TPA cross sections for derivatives bearing dialkylamino donating groups occur at the shortest wavelength of the excitation region, i.e. 750 nm, and lie in the range 286−807 GM. The TPA maximum wavelength (λ_{TPA}) is thus less than twice that of the single photon absorption (otherwise a strong band at ca. 800 nm should appear), proving a quadrupolar character of the chromophores **1** and **2** in spite of the unsymmetrical nature of the benzothiazole itself. In contrast, the derivatives containing diphenylamino electron-donating functionality exhibit somewhat higher values of δ_{TPA} and the position of the maxima is shifted to longer wavelengths, namely to 760 (**1b**) and 800 nm (**2b**). The highest TPA cross-section is exhibited by compound **2b** and is as large as 1110 GM. The results of TPA measurements have also shown that alkene π-bridged chromophores have somewhat superior TPA properties over their alkyne π-bridged counterparts. However, the TPA activity of the triple-bond analogue **1b** does not differ too much from that of **2b** (δ_{TPA} is ca. 1.2 times smaller), and since the quantum yield of **1b** is considerably higher (0.57 vs 0.43), compound **1b** could be viewed as a suitable candidate for practical applications as well.

TABLE 3. Calculated TPA Cross Sections for the First Three Excitations Using Quadratic Response Function

system	n	B3LYP/6-31G(d)			CAM-B3LYP/6-31G(d)		
		E_{max} [eV]	λ_{TPA} [nm]	δ_{TPA} [GM]	E_{max} [eV]	λ_{TPA} [nm]	δ_{TPA} [GM]
1a	1	2.83	876	250	3.39	732	11
	2	3.34	743	2084	4.10	605	868
	3	3.93	631	324	4.49	552	339
1b	1	2.64	939	301	3.27	758	2
	2	2.99	829	3239	3.82	649	962
	3	3.55	699	720	4.39	565	904
2a	1	2.68	925	262	3.22	770	10
	2	3.18	780	2104	3.95	628	874
	3	3.69	672	158	4.39	565	1052
2b	1	2.50	992	284	3.12	795	2
	2	2.85	870	3422	3.70	670	1043
	3	3.35	740	592	4.26	582	1954
3	1	2.61	950	13	3.19	777	4
	2	2.94	844	3673	3.72	667	522
	3	3.33	745	1235	4.38	566	116
4	1	2.63	943	13	3.20	775	4
	2	2.97	835	3393	3.73	665	372
	3	3.22	770	97	3.84	646	92

To investigate these results more thoroughly, quantum-chemical calculations of the TPA cross sections were performed. Here, it is worth noting that although calculations with DFT methods somehow overestimate δ_{TPA} values, they can nevertheless provide the correct structure-to-property relations for TPA processes, as has been shown in previous systematic studies.[14,43]

The TPA cross sections δ_{TPA} calculated by using the response theory for the first three excited states are collected in Table 3. It can be seen that the maximum TPA cross-section corresponds in most cases to the excitation from the ground state to the second excited state ($S_0 \rightarrow S_2$). This transition takes place from both HOMO-1 and HOMO to the LUMO and LUMO$+1$, and is associated with a charge-transfer process from both donor edges to the benzothiazole core. The TPA cross sections associated with the $S_0 \rightarrow S_1$ transition, which has the largest transition dipole moment and appears as the strongest absorption band in the VIS spectra, are more than 1 order of magnitude smaller. This is consistent with the selection rules for allowed and not-allowed transitions in quadrupolar molecules, which are opposite for one- and two-photon absorption.[44]

Since the solvent has a significant impact on the TPA cross sections, calculations of δ_{TPA} using the solvation model were carried out as well (cf. Table S2, Supporting Information). In general, δ_{TPA} values corresponding to the $S_0 \rightarrow S_2$ excitations are approximately 1.5 times larger than those in vacuo, but the relative trends remain essentially unchanged. The effects of the vibronic coupling on the TPA cross sections were neglected in this study, as they tend to be very small for one-dimensional conjugated systems.[45]

A deeper insight into the origin of the large TPA cross sections was obtained by using the three-state model:[46]

$$\delta_{fg} \propto \left[\frac{|\mu_{fk}|^2 |\mu_{kg}|^2}{\left(\frac{E_{kg}}{E_{fg}} - \frac{1}{2} \right)^2} + 4|\mu_{fg}|^2 |\Delta\mu_{fg}|^2 \right] \frac{1}{\Gamma_{fg}}$$

where only one intermediate state (k) beside the ground (g) and final (f) states is taken into account. Here, E_{lm} and μ_{lm} are the transition energy and the transition dipole moments between states l and m (l, m = f, k, g), respectively, $\Delta\mu_{fg}$ is the dipole moment difference between states f and g, and Γ_{fg} is the damping factor in units of energy. In many publications, one of the two terms in the square brackets is omitted, depending on the symmetry of the studied molecular structures. Due to its simplicity, this model is widely used for rationalization of calculated TPA values in terms of one-photon excitation characteristics, although it may fail in certain cases. The estimated values of δ_{TPA} using the three-state model are shown in Table 2. In the present investigation, a direct comparison of δ_{TPA} values of selected chromophores is used to discuss some structural aspects that influence the TPA properties.

Effect of Donor Strength/Ability. As already mentioned above, the derivatives bearing diarylamino functionality display higher δ_{TPA} values compared to their dialkylamino counterparts. This corresponds with a stronger donor ability of the diphenylamino moiety, which is more electron-rich than a dialkylamino group (cf. Tables S3 and S4, Supporting Information). However, the experimental TPA enhancement factor of ca. 2 to 3 for the couples of **2a/2b** and **1a/1b**, respectively (cf. Table 1), is larger than the predicted values of 1.2 (CAM-B3LYP) and 1.6 (B3LYP). It should be noticed that these calculated factors are almost unaffected by the solvation model (cf. Table S2, Supporting Information). The overestimation of the experimental factors can be mostly attributed to the fact that the δ_{TPA} values measured at 750 nm for **1a** and **2a** are off-resonant maxima, and therefore it is difficult to compare them directly with the calculated values. The wavelength λ_{TPA} associated with half the second excitation energy ($E_{max,2}/2$) as calculated by the CAM-B3LYP method for dialkylamino derivatives is far below 750 nm. Therefore, the δ_{TPA} as a function of wavelength decreases within the measurement range 750–840 nm and does not cover any clearly defined maxima. The energy of the second excited state for derivatives, where the dialkylamino functionality is replaced by a diphenylamino group, is substantially red-shifted (cf. Table 3) and the maximum δ_{TPA} values are predicted at longer wavelengths, as confirmed experimentally. For a quantitative comparison, one should, however,

(43) Baev, A.; Prasad, P. N.; Samoc, M. *J. Chem. Phys.* **2005**, *122*, 224309. Badaeva, E. A.; Timofeeva, T. V.; Masunov, A. M.; Tretiak, S. *J. Phys. Chem. A* **2005**, *109*, 7276–7284. Rubio-Pons, O.; Luo, Y.; Agren, H. *J. Chem. Phys.* **2006**, *124*, 94310. Salek, P.; Vahtras, O.; Guo, J. D.; Luo, Y.; Helgaker, T.; Agren, H. *Chem. Phys. Lett.* **2003**, *374*, 446–452. Ferrighi, L.; Frediani, L.; Fossgaard, E.; Ruud, K. *J. Chem. Phys.* **2007**, *127*, 244103. Day, P. N.; Nguyen, K. A.; Pachter, R. *J. Chem. Phys.* **2006**, *125*, 094103. Katan, C.; Tretiak, S.; Werts, M. H. V.; Bain, A. J.; Marsh, R. J.; Leonczek, N.; Nicolaou, N.; Badaeva, E.; Mongin, O.; Blanchard-Desce, M. *J. Phys. Chem. B* **2007**, *111*, 9468–9483.

(44) Molecules under study are so-called quasi-quadrupolar systems because of their nonzero-ground-state dipole moments. Therefore the selection rules are not as straightforward.

(45) Luo, Y.; Agren, H.; Knuts, S.; Jorgensen, P. *Chem. Phys. Lett.* **1993**, *213*, 356–362. Macak, P.; Luo, Y.; Agren, H. *Chem. Phys. Lett.* **2000**, *330*, 447–456. Macak, P.; Luo, Y.; Norman, P.; Agren, H. *J. Chem. Phys.* **2000**, *113*, 7055–7061.

(46) Pond, S. J. K.; Rumi, M.; Levin, M. D.; Parker, T. C.; Beljonne, D.; Day, M. W.; Bredas, J. L.; Marder, S. R.; Perry, J. W. *J. Phys. Chem. A* **2002**, *106*, 11470–11480. Day, P. N.; Nguyen, K. A.; Pachter, R. *J. Phys. Chem. B* **2005**, *109*, 1803–1814. Ohta, K.; Antonov, L.; Yamada, S.; Kamada, K. *J. Chem. Phys.* **2007**, *127*, 084504.
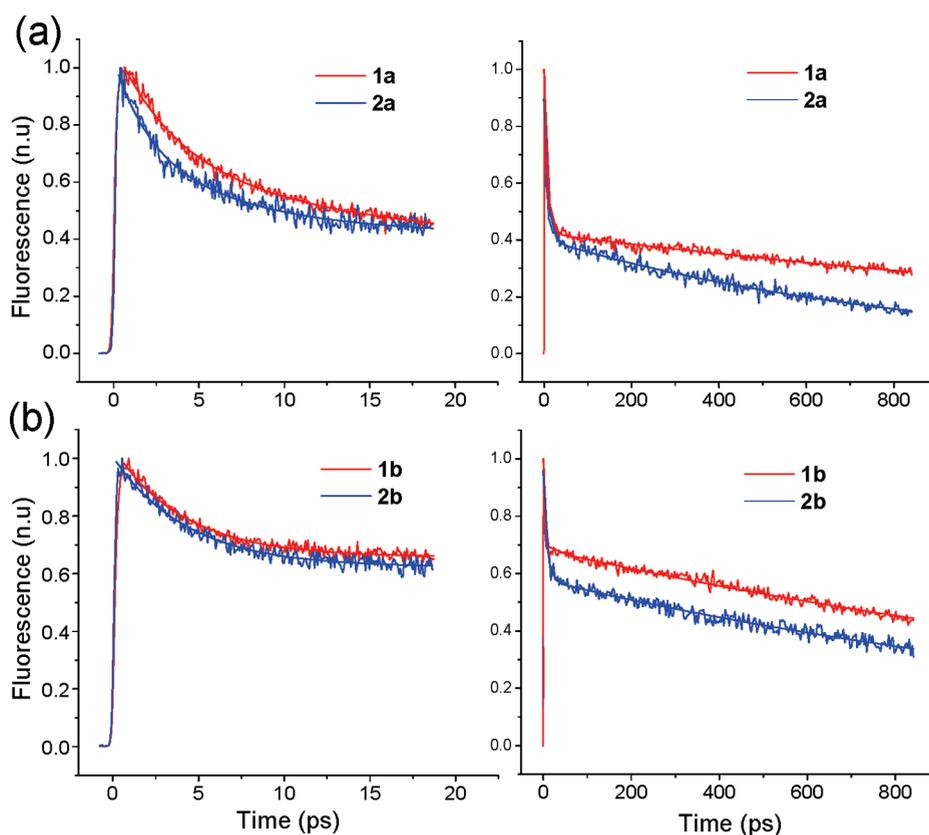
FIGURE 6. Fluorescence dynamics (at the excitation wavelength 400 nm) in short (left) and long (right) time scales of (a) **1a** and **2a** and (b) **1b** and **2b**. The decays were detected at the peak of the fluorescence spectrum of each compound.

keep in mind that excitation energies are somewhat overestimated (underestimated) with the CAM-B3LYP (B3LYP) method. The higher TPA activity of **1b** and **2b** with respect to **1a** and **2a** can be ascribed to a larger transition dipole moment μ_{01} as well as to a larger excited-to-excited transition moment μ_{12} (cf. Table 2).

At this stage, it is not clear why the compound **1d** has an approximately two times higher TPA cross-section than its analogues **1a** and **1c**, despite their similar one-photon excitation properties. Such an outcome can be presumably attributed to the interaction of the polar hydroxy groups with the solvent and a somewhat different relaxed conformation in the excited state.

Effect of π-Bridging. Regarding Table 1, it is evident that compounds **2a** and **2b** containing ethenylene spacers exhibit larger TPA cross sections (by 2.1 and 1.2 times, respectively) than their ethynylene π-bridged counterparts **1a** and **1b**. Although this finding is qualitatively consistent with the δ_{TPA} values evaluated from the quadratic response function, the theoretically predicted differences between systems containing ethynylene and ethenylene linkages are notably smaller (cf. Table 3). Similar small changes in TPA activity have also been reported theoretically for other quadrupolar molecules.[31,47] As one can notice from Table 2, within these respective (alkene and alkyne π-bridged) series, there is no significant change in the transition dipole moments μ_{01} and μ_{12}. Furthermore, use of the three-state model even results in

opposite trends with respect to a π-bridge used in the conjugation (cf. Table 2).

Recently, Bhaskar et al.[8] have explained the higher TPA cross sections of branched alkene chromophores compared to their alkyne counterparts by using time-resolved measurements. These measurements have revealed a greater amount of charge transfer in alkene π-bridged systems by virtue of a greater population of the conformationally and solvent relaxed ICT state. To prove this assumption and gain a better insight into this problem, time-resolved fluorescence measurements of benzothiazole dyes in short and long time scales were also performed. The results are shown in Figure 6.

All the studied compounds exhibit a biexponential decay with a fast mechanism of a few picoseconds followed by a slower one in the nanosecond time scale. The fast fluorescence decay mechanism could be attributed to relaxation from the locally excited state toward an intramolecular charge transfer (ICT) state.[48] The formation of an ICT state is accompanied by a charge-transfer process from the electron-donating edge substituents to the electron-accepting core. In compounds containing ethenylene spacer the relaxation toward ICT is faster and more efficient than that in those containing ethynylene spacer. This is obvious in both short- and long-scale results. Specifically, the time constants of the fast decays are 2.0, 3.6, 3.8, and 4.3 ps for **2a**, **1a**, **2b**, and **1b**, respectively. The faster relaxation toward the ICT state in alkene π-bridged compounds can be an indication that the

(47) Lee, J. Y.; Kim, K. S.; Mhin, B. J. *J. Chem. Phys.* **2001**, *115*, 9484–9489.

(48) Yan, Y. L.; Li, B.; Liu, K. J.; Dong, Z. W.; Wang, X. M.; Qian, S. X. *J. Phys. Chem. A* **2007**, *111*, 4188–4194. Li, B.; Tong, R.; Zhu, R. Y.; Meng, F. S.; Tian, H.; Qian, S. X. *J. Phys. Chem. B* **2005**, *109*, 10705–10710.

charge transfer is more efficient than in those with alkyne π-bridge.[8] As the charge transfer in the excited state plays a vital role in increasing the TPA cross-section, greater population of the ICT state for the alkene π-bridged system could be the reason why these compounds are more efficient TPA materials. Additionally, the faster relaxation dynamics of the alkene π-bridged compounds, **2a** and **2b**, agrees well with their lower quantum yield values compared to the alkyne ones, **1a** and **1b**.

Effect of Central Core. To assess the effect of central core on the TPA properties, we compared the TPA cross-section of **2b** with those of its two analogues **3** and **4**, where the benzothiazole moiety is replaced by a fluorene and a carbazole, respectively. These systems were experimentally studied recently and more details can be found in ref 12. While the fluorene serves as a π-conjugated center, carbazole can be assumed as an electron-donating π-center. From the experimental data presented in Table 1, it is obvious that the benzothiazole-based dye **2b** is markedly superior to those derived from fluorene or carbazole. Specifically, the TPA cross-section of **2b** is two-times larger than the δ_{TPA} value of **3** and more than 1 order of magnitude larger compared to that of **4**. Indeed, this result is consistent with the nature of the central core and can be intuitively understood as follows: Electron-rich carbazole hinders an electron transfer from donor edges to the central core and dramatically reduces charge transfer efficiency. On the other hand, the electron-withdrawing benzothiazole pulls electron density toward itself and enhances charge transfer efficiency, resulting in a better performance of the systems with the D-π-A-π-D backbone in comparison with those of D-π-D or D-π-D-π-D type. The benzothiazole unit can thus serve as an alternative and very efficient π-center in TPA chromophores with electron-donating edge substituents.

Surprisingly, the widely used B3LYP method provides incorrect trends in the predicted δ_{TPA} values (cf. Table 3) and thus is not capable of reproducing the experimentally observed features within this series, presumably due to an incorrect asymptotic behavior of the exchange-correlation potential.[14,49] The correct trends are, however, recovered by using the Coulomb-attenuated CAM-B3LYP functional, which to a large extent remedies the difficulties of standard DFT in the description of charge-transfer processes. By using the three-state model and one-photon absorption characteristics presented in Table 2, the much larger TPA cross-section of **2b** with respect to those of **3** and **4** can be rationalized by its significantly higher value of the transition dipole moment from the first to the second excited state μ_{12}. The overestimation of μ_{12} values for fluorene and carbazole-derived dyes at the B3LYP level of theory is apparently the major source for the discrepancy between the experimentally observed trends and those obtained by using the B3LYP method (cf. Table S1, Supporting Information).

Conclusions

A series of novel quasi-quadrupolar fluorophores of D-π-A-π-D type containing benzothiazole as the central electron-withdrawing core have been synthesized and characterized.

Fast and effective access to the target compounds with ethynylene spacers (**1a**−**d**) was accomplished through a double Sonogashira-type cross-coupling reaction between 2,6-diiodobenzothiazole and the corresponding 4-donor-substituted phenylacetylenes. Two analogues with ethenylene linkage (**2a,b**) were obtained via a palladium-catalyzed Suzuki coupling, followed by an aldol-type condensation. Several methodologies for the synthesis of 4-donor-substituted phenylacetylenes were compared, and facile synthetic routes to 4-(diphenylamino)phenylacetylene (**7b**) and hitherto unknown 2,6-diiodobenzothiazole (**5**), as valuable building blocks, were developed.

The title compounds prepared in this work were investigated both experimentally and theoretically in detail for their linear and nonlinear optical properties. All molecules under study absorb in the violet region and emit light in the blue-green spectral region. The substitution of a dialkylamino group for a diarylamino one gives only a minimal difference in the excitation energies. A more pronounced red-shift of the absorption and fluorescence maxima is achieved by the replacement of ethynylene linkages with ethenylene ones. This change, however, results in smaller fluorescence quantum yields.

The TPA cross sections obtained by the two-photon induced fluorescence measurement in the femtosecond time domain confirm a quadrupolar character of the studied compounds and the superiority of alkene over alkyne π-bridge in these systems. In general, the maximum TPA cross sections of derivatives bearing diphenylamino electron-donating functionalities are higher and occur at longer wavelengths compared to their dialkylamino counterparts. Comparison of the TPA cross section of **2b** with analogous dyes containing fluorene or carbazole as the central core sustains the benzothiazole-derived dye as markedly superior. This in turn implies higher efficiency of the D-π-A-π-D-type structures in terms of TPA over those of D-π-D or D-π-D-π-D type. It is also worth noting that the experimentally determined δ_{TPA} values of **1b** and **2b** are comparable to or in most cases even larger than those of previously reported benzothiazole-containing dyes.

Quantum chemical calculations of the TPA cross sections with use of the quadratic response time-dependent DFT with the CAM-B3LYP functional clearly support the experimentally observed trends. Nevertheless, the failure of the widely used B3LYP method for the prediction of TPA activities within the series with varying central cores was demonstrated. This indicates better suitability of the former method for a reliable computer-aided design of TPA dyes.

In conclusion, the benzothiazole derivatives **1** and **2** prepared herein represent the first examples of TPA dyes containing the benzothiazole unit as the electron-withdrawing π-center, and in principle could provide a useful guideline to the design of novel heterocycles-based TPA molecules. Suitable one- and two-photon absorption and emission properties combined with their relatively small size and a high chemical and photophysical stability make the title fluorophores promising for optoelectronic applications. Additional modification of the title structures by quaternization or metal complexation of the benzothiazole nitrogen might open an avenue for the preparation of novel highly efficient ionic dyes with reasonable water solubility and enhanced TPA properties.

(49) Peach, M. J. G.; Helgaker, T.; Salek, P.; Keal, T. W.; Lutnaes, O. B.; Tozer, D. J.; Handy, N. C. *Phys. Chem. Chem. Phys.* **2005**, *8*, 558–562.

Experimental Section

I. Synthetic Procedures. 2-Amino-6-bromobenzothiazole (16b). A mixture of 4-bromoaniline (0.5 g, 2.9 mmol) and NH₄SCN (1.1 g, 14.5 mmol) in glacial acetic acid (5 mL) was cooled and stirred. To this solution was added bromine (0.2 mL, 3.8 mmol) dissolved in acetic acid (1.5 mL) at such a rate to keep the temperature below 15 °C throughout the addition. Stirring at 15−18 °C was continued for an additional 3 h, then the reaction mixture was poured into water, neutralized with a 25% aqueous solution of NH₄Cl, and extracted with ethyl acetate (3 × 15 mL). The combined organic layers were dried over Na₂SO₄ and solvents were evaporated. The crude product was purified by column chromatography on silica gel (eluent hexanes/EtOAc = 1:1) to yield the title compound (0.5 g; 75%) as a pale yellow solid. R_f 0.67 (SiO₂, hexanes/EtOAc = 1:1); mp 213−214 °C (lit.[36] mp 215−217 °C); ¹H NMR (300 MHz, CDCl₃) δ 7.83−7.37 (m, 3H, H$_{ar}$), 5.44 (br s, 2H, NH₂).

2,6-Dibromobenzothiazole (6). 2-Amino-6-bromobenzothiazole (16b) (0.5 g, 2.2 mmol) was mixed under intensive stirring with 85% phosphoric acid (5 mL) at 50 °C. The solution was cooled to −20 °C and a solution of sodium nitrite (0.18 g, 2.6 mmol) in water (1 mL) was added slowly, maintaining the temperature in the range −15 to −10 °C. After 1 h of stirring at −10 °C, the resulting diazonium salt was poured over a solution of active copper(I) bromide (0.41 g, 2.86 mmol) in 48% HBr (2.5 mL) and intensively stirred for 1 h at room temperature. Consequently, the mixture was heated at 40 °C for 2 h and then stirred at rt overnight. The reaction mixture was diluted to a final volume of 150 mL and extracted with CH₂Cl₂ (5 × 30 mL). The combined organic extracts were dried over Na₂SO₄, the solvent was removed, and the crude product was purified by column chromatography on silica gel (eluent chloroform/hexanes = 1:1) to yield **6** (0.45 g; 70%) as a white solid. R_f 0.21 (SiO₂, chloroform/hexanes = 1:1); mp 118−120 °C (lit.[50] mp 119−121 °C); ¹H NMR (300 MHz, CDCl₃) δ 7.95 (d, J = 2.0 Hz, 1H, H-7), 7.84 (d, J = 8.7 Hz, 1H, H-4), 7.58 (dd, J = 8.7, 2.0 Hz, 1H, H-5); ¹³C NMR (75 MHz, CDCl₃) δ 151.2, 139.4, 138.8, 130.2, 123.9, 123.4, 119.6.

6-Iodobenzothiazole-2-thiol (18). To a solution of 6-amino-benzothiazole-2-thiol (2.7 g, 15 mmol) in a 5% aqueous solution of NaOH (10 mL) was added sodium nitrite (25% aqueous solution, 10 mL). The resulting mixture was added dropwise, with cooling (0−5 °C) and stirring, to concentrated hydrochloric acid (50 mL). A solution of the resulting diazonium salt was added dropwise under stirring to a solution of potassium iodide (3 g, 18 mmol) in 50 mL of water and the resulting mixture was heated in an oil bath at 100 °C for 1 h. After standing for 24 h at room temperature, the separated (6-iodo-2-benzothiazolyl) disulfide was filtrated, washed with water until neutral, and mixed with a solution of Na₂S·9H₂O (10 g, 42 mmol) in 120 mL of water. The mixture was heated at 80 °C for 4 h while a continued stream of hydrogen sulfide was passed through it. The solution was filtered and acidified with 30−50% acetic acid. The separated solid was isolated then dissolved in 10−15% aqueous ammonia solution, and after filtration acetic acid was again added to the solution. The precipitated 6-iodobenzothiazole-2-thiol (2.24 g, 51%) was crystallized from the ethanol/chloroform (1:1) mixture. Mp 268−270 °C (lit.[51] mp 267−269 °C); ¹H NMR (300 MHz, CDCl₃) δ 13.84 (br s, 1H, SH), 8.10 (d, J = 1.3 Hz, 1H, H-7), 7.70 (dd, J = 8.4, 1.6 Hz, 1H, H-5), 7.09 (d, J = 8.4 Hz, 1H, H-4); ¹³C NMR (75 MHz, CDCl₃) δ 190.5, 141.4, 136.0, 132.1, 130.2, 114.6, 88.6.

2-Chloro-6-iodobenzothiazole (19). To a solution of 6-iodo-benzothiazole-2-thiol (3.0 g, 10 mmol) in CH₂Cl₂ (6 mL), cooled in an ice−water bath, was added SO₂Cl₂ (6 mL, 37 mmol) under nitrogen, and the suspension was stirred at room temperature for 4 h. Consequently, ice water was carefully added to the reaction mixture under cooling and continuous stirring (exothermic reaction, foaming occurred). A yellow precipitate was formed immediately, and stirring was continued for 2 h. The solid precipitate was collected by filtration then washed with water and the crude product was purified by column chromatography on silica gel (eluent chloroform/hexanes = 2:1) to yield 2-chloro-6-iodobenzothiazole (2.0 g, 66%) as a white solid. R_f 0.44 (SiO₂, CHCl₃/hexanes = 2:1); mp 135−137 °C (lit.[52] mp 137 °C); ¹H NMR (300 MHz, CDCl₃) δ 8.12 (d, J = 1.7 Hz, 1H, H-7), 7.78 (dd, J = 8.5, 1.7 Hz, 1H, H-5), 7.68 (d, J = 8.5 Hz, 1H, H-4); ¹³C NMR (75 MHz, CDCl₃) δ 150.8, 150.3, 137.9, 135.9, 129.6, 124.3, 90.1.

2,6-Diiodobenzothiazole (5). To a solution of 2-chloro-6-iodobenzothiazole (2.0 g, 6.76 mmol) in dry chloroform (25 mL), freshly distilled from CaCl₂, was added dry NaI (5.0 g, 34 mmol). The suspension was stirred at room temperature for 15 min, and then acetyl chloride (2.4 mL, 34 mmol) was added. The reaction mixture was stirred at room temperature for 10 min, and consequently neutralized with a saturated aqueous solution of K₂CO₃. Afterward, 20% aqueous solution of Na₂S₂O₅ was added until the organic layer became colorless. The reaction mixture was extracted with chloroform (3 × 20 mL), combined organic layers were dried over Na₂SO₄, and chloroform was evaporated. The crude product was purified by column chromatography on silica gel (eluent chloroform/hexanes = 1:1) to yield the title compound (1.3 g, 50%) as a white solid. R_f 0.19 (SiO₂, chloroform/hexanes = 1:1); mp 101−103 °C; ¹H NMR (300 MHz, CDCl₃) δ 8.20 (d, J = 1.3 Hz, 1H), 7.75 (s, 1H), 7.74 (d, J = 1.3 Hz, 1H); ¹³C NMR (75 MHz, CDCl₃) δ 153.6, 141.1, 135.5, 128.9, 123.8, 106.2, 90.6. Anal. Calcd for C₇H₃I₂NS: C 21.73, H 0.78, N 3.62. Found: C 21.97, H 0.59, N 3.88.

6-Nitro-2-methylbenzothiazole (21). 2-Methylbenzothiazole (20) (14.9 g, 0.1 mol) was dissolved under vigorous stirring in concd H₂SO₄ (60 mL). The solution was cooled to 0 °C and the nitration mixture (15 mL 100% HNO₃ and 10 mL concd H₂SO₄) was added dropwise at such a rate to keep the temperature below 5 °C throughout the addition. After the addition was completed, the reaction mixture was stirred under cooling for 15 min and then at room temperature for a further 2 h. Subsequently, the mixture was poured into ice-cold water (400 mL). The precipitate was collected by filtration, washed with cold water until the pH was neutral, and crystallized from 80% ethanol to give the title compound in 76% yield (14.8 g). Mp 166−167 °C (lit.[53] mp 166.5−167.5 °C); ¹H NMR (300 MHz, CDCl₃) δ 8.78

(50) Elderfield, R. C.; Short, F. W. *J. Org. Chem.* **1953**, *18*, 1092−1103.

(51) Mikulasek, S.; Sutoris, V.; Foltinova, P.; Konecny, V.; Blockinger, G. *Chem. Zvesti* **1974**, *28*, 686−692.

(52) Drozdov, N. S.; Stavrovskaya, V. I. *Zh. Obshch. Khim.* **1939**, *9*, 409−414.

(53) Santos, P. F.; Reis, L. V.; Duarte, I.; Serrano, J. P.; Almeida, P.; Oliveira, A. S.; Ferreira, L. F. V. *Helv. Chim. Acta* **2005**, *88*, 1135−1143.

(d, J = 2.4 Hz, 1H, H-7), 8.34 (dd, J = 9.0 Hz, 2.4 Hz, 1H, H-5), 8.04 (d, J = 9.0 Hz, 1H, H-4), 2.92 (s, 3H, CH$_3$).

6-Amino-2-methylbenzothiazole (22). To a mixture of 6-nitro-2-methylbenzothiazole (**21**) (3 g, 15 mmol) and concd hydrochloric acid (9 mL, 44 mmol) in 80% ethanol (200 mL) was added powdered iron (3.88 g, 70 mmol). The reaction mixture was sonicated for 40 min (temperature was attained at 90 °C) and then cooled to room temperature. Precipitated iron oxides were removed by filtration through a short pad of silica gel and washed with ethanol (2 × 30 mL). The solvent was removed and the solid residue was extracted into a heterogeneous mixture of EtOAc and 10% aq solution of Na$_2$CO$_3$. The organic layer was dried (Na$_2$SO$_4$) and the solvent was removed under vacuum. The crude product was purified by short-column chromatography on silica gel (eluent hexanes/EtOAc = 2:1) to yield **22** (2.33 g, 92%) as a white solid. R_f 0.11 (SiO$_2$, hexanes/EtOAc = 1:1); mp 125–126 °C (lit.[24] mp 125–126 °C); ^{1}H NMR (300 MHz, CDCl$_3$) δ 7.70 (d, J = 8.8 Hz, 1H, H-4), 7.06 (d, J = 2.8 Hz, 1H, H-7), 6.79 (dd, J = 8.8, 2.8 Hz, 1H, H-5), 3.78 (s, 2H, NH$_2$), 2.75 (s, 3H, CH$_3$).

6-Iodo-2-methylbenzothiazole (8). To a cooled solution of **22** (2 g, 12 mmol) in concd HCl (7 mL) and water (7 mL) was added a solution of sodium nitrite (1.66 g, 24 mmol) in water (2 mL) dropwise, maintaining the reaction temperature in the range 0 to 5 °C. After 1 h of stirring at −5 °C, a solution of KI (3.98 g, 24 mmol) in H$_2$O (5 mL) was added dropwise. After 30 min of stirring, the temperature was allowed to rise gradually to room temperature and the reaction mixture was intensively stirred for 1 h. Afterward the reaction mixture was poured into cold water then extracted with CH$_2$Cl$_2$ (5 × 30 mL) and the combined organic layers were washed with a 5% aqueous solution of Na$_2$SO$_3$. After drying over Na$_2$SO$_4$ and evaporation of the solvent, the crude product was purified by column chromatography on silica gel (eluent CH$_2$Cl$_2$) to yield **8** as a white solid (1.32 g, 40%). R_f 0.53 (SiO$_2$, CH$_2$Cl$_2$); mp 140–142 °C (lit.[53] mp 140–141 °C); ^{1}H NMR (300 MHz, CDCl$_3$) δ 8.16 (d, J = 1.6 Hz, 1H, H-7), 7.73 (dd, J = 1.6 Hz, 8.4 Hz; 1H, H-5), 7.67 (d, J = 8.4 Hz, 1H, H-4), 2.82 (s, 3H, CH$_3$); ^{13}C NMR (75 MHz, CDCl$_3$) δ 162.3, 147.6, 132.6, 129.8, 124.6, 118.7, 83.7, 14.8.

N,N-(Diphenylamino)benzaldehyde (10b). POCl$_3$ (1.6 mL, 16.3 mmol) was added slowly to dry DMF (20 mL) under cooling and intensive stirring. The stirring was continued for 15 min, and then the temperature was allowed to rise to 30 °C. Triphenylamine (2.0 g, 8.15 mmol) was added slowly, and the reaction mixture was stirred at 90–100 °C for 3 h. After cooling to room temperature, the mixture was poured into a mixture of water (150 mL) and ice (50 g), then neutralized with a 20% aqueous solution of sodium carbonate. A pale yellow precipitate was collected by filtration, washed with cold water and 20% ethanol, and purified by column chromatography on silica gel (eluent hexanes/EtOAc = 4:1) to yield **10b** (1.9 g, 85%) as a pale yellow solid. R_f 0.92 (SiO$_2$, hexanes/EtOAc = 4:1); mp 132–133 °C (lit.[54] mp 132–134 °C); ^{1}H NMR (300 MHz, CDCl$_3$) δ 9.81 (s, 1H, CHO), 7.67 (d, J = 8.8 Hz, 2H), 7.34 (t, J = 7.7 Hz, 4H), 7.10–7.16 (m, 6H), 7.01 (d, J = 8.8 Hz, 2H).

General Procedure for the Preparation of Terminal Acetylenes 7a and 7c,d. Method A: To a mixture of 4-iodo-N,N-

dialkylaniline (**11a**, **11c**, or **11d**, 10 mmol), Pd(PPh$_3$)$_2$Cl$_2$ (0.35 g, 0.5 mmol), and copper iodide (38 mg, 0.2 mmol) was added THF (30 mL) under nitrogen, and the suspension was stirred at room temperature for 15 min. Consequently, triethylamine (7 mL), freshly distilled from CaH$_2$, was added. After stirring for 30 min at room temperature, trimethylsilylacetylene (1.9 mL, 13 mmol) was added dropwise. The reaction mixture was stirred under nitrogen at room temperature for 24 h, and then at 50 °C for a further 3 h. After this time, the reaction mixture was diluted with Et$_2$O and filtered through a short column of silica, eluting with hexanes/EtOAc = 1:1. The solvents were removed and the crude intermediate was used in the next step without further purification.

To a solution of trimethylsilyl intermediate (10 mmol) in 20 mL of THF, cooled to 0 °C, was added 10 mL of 1 M solution of tetrabutylammonium fluoride (10 mmol) in THF dropwise. The reaction mixture was stirred at 0 °C for 3 h and then absorbed onto silica gel. The title compounds were obtained by column chromatography on silica gel (eluent hexanes/EtOAc = 5:1 to 3:1) in yields as follows: **7a** (1.1 g, 75%), **7c** (2.0 g, 70%), and **7d** (1.5 g, 74%).

Method B:. 3-(4-Dialkylaminophenyl)prop-2-yn-1-ol (12a, 12c) To a mixture of 4-iodo-N,N-dialkylaniline (20 mmol), Pd(PPh$_3$)$_2$Cl$_2$ (213 mg, 0.3 mmol), and copper iodide (38 mg, 0.2 mmol) was added triethylamine (20 mL, freshly distilled from CaH$_2$) under nitrogen. After stirring for 30 min at room temperature, propargyl alcohol (1.53 mL, 26 mmol) was added dropwise. The reaction mixture was stirred under nitrogen at room temperature for 24 h. Then the precipitate was collected by filtration and washed with ether and solvents were evaporated. The crude product was purified by column chromatography on silica gel (eluent hexanes/EtOAc = from 2:1 to 1:1) to yield the title compounds **12a** and **12c**.

12a: 2.76 g (78%); pale brown solid; R_f 0.36 (SiO$_2$, hexanes/EtOAc = 2:1); mp 53–55 °C (lit.[55] mp 51.2–53.7 °C); ^{1}H NMR (300 MHz, CDCl$_3$) δ 7.30 (d, J = 8.9 Hz, 2H, H$_{ar}$), 6.60 (d, J = 8.9 Hz, 2H, H$_{ar}$), 4.45 (d, J = 4.1 Hz, 2H, CH$_2$–O), 2.95 (s, 6H, NMe$_2$), 1.30 (br s, 1H, OH).

12c: 5.3 g (84%); brown oil; R_f 0.41 (SiO$_2$, hexanes/EtOAc = 1:1); ^{1}H NMR (300 MHz, CDCl$_3$) δ 7.31 (d, J = 9.1 Hz, 2H, H$_{ar}$), 6.67 (d, J = 9.1 Hz, 2H, H$_{ar}$), 4.47 (d, J = 5.1 Hz, 2H, CH$_2$–OH), 4.23 (t, J = 6.3 Hz, 4H, 2 × CH$_2$–O), 3.63 (t, J = 6.3 Hz, 4H, N–CH$_2$), 2.04 (s, 6H, 2 × CH$_3$), 1.26 (t, J = 5.1 Hz, 1H, OH).

4-(N,N-Dimethylamino)phenylacetylene (7a). Compound **12a** (1.75 g, 0.01 mol) was dissolved in THF (30 mL), followed by an addition of active MnO$_2$ (4.35 g, 0.05 mol) and powdered potassium hydroxide (2.8 g, 0.05 mol). The reaction mixture was stirred at room temperature for 6 h and consequently filtrated through a short column of silica. The solid part was washed with CHCl$_3$ (50 mL), solvent from combined organic layers was evaporated, and the crude product was purified by column chromatography on silica gel (eluent hexanes/EtOAc = 6:1) to yield 72% (1.05 g) of **7a** as a white solid. R_f 0.55 (SiO$_2$, hexanes/EtOAc = 6:1); mp 52–53 °C (lit.[56] mp 51–52 °C); ^{1}H NMR (300 MHz, CDCl$_3$)

(54) Kauffman, J. M.; Moyna, G. *J. Org. Chem.* **2003**, *68*, 839–853.

(55) LaClair, J. J. *J. Am. Chem. Soc.* **1997**, *119*, 7676–7684.
(56) Rodriguez, J. G.; Tejedor, J. L.; Rumbero, A.; Canoira, L. *Tetrahedron* **2006**, *62*, 3075–3080.

δ 7.36 (d, J = 9.1 Hz, 2H, H$_{ar}$), 6.61 (d, J = 8.9 Hz, 2H, H$_{ar}$), 2.97 (br s, 7H, C≡CH, NMe$_2$).

3-{4-[*N*,*N*-Bis(2-acetoxyethyl)amino]phenyl}prop-2-yn-1-al (13c). Starting compound **12c** (2.0 g, 6.27 mmol) was dissolved in THF (35 mL), active manganese dioxide (5.45 g, 60 mmol) was added, and the suspension was stirred at room temperature for 24 h. The reaction mixture was filtered through a short column of SiO$_2$, and the solid part was washed with ether (20 mL) and chloroform (20 mL). After evaporation of solvents the crude product was purified by column chromatography (SiO$_2$, eluent CHCl$_3$/CH$_3$OH = 30:1) to yield the title compound as a brown oil (1.3 g, 67%). R_f 0.55 (SiO$_2$, CHCl$_3$/CH$_3$OH = 30:1); ^{1}H NMR (300 MHz, CDCl$_3$) δ 9.37 (s, 1H, CH═O), 7.49 (d, J = 9.1 Hz, 2H, H$_{ar}$), 6.74 (d, J = 9.1 Hz, 2H, H$_{ar}$), 4.26 (t, J = 6.0 Hz, 4H, CH$_2$–O), 3.68 (t, J = 6.0 Hz, 4H, N–CH$_2$), 2.05 (s, 6H, 2 × CH$_3$).

4-[*N*,*N*-Bis(2-acetoxyethyl)amino]phenylacetylene (7c). Compound **13c** (1.9 g, 6 mmol) was dissolved in dry THF (25 mL), powdered potassium hydroxide (1.7 g, 30 mmol) was added, and the reaction mixture was stirred at room temperature for 4 h and then at 50 °C for a further 5 h. The solid part was filtered off through a short column of SiO$_2$ and washed with CHCl$_3$ (50 mL). Organic solvents were evaporated and the product was obtained by column chromatography (SiO$_2$, eluent hexanes/EtOAc = 2:1) in 90% yield (1.56 g). R_f 0.43 (SiO$_2$, hexanes/EtOAc = 2:1); mp 45−47 °C; ^{1}H NMR (300 MHz, CDCl$_3$) δ 7.36 (d, J = 9.1 Hz, 2H, H$_{ar}$), 6.68 (d, J = 9.1 Hz, 2H, H$_{ar}$), 4.24 (t, J = 6.3 Hz, 4H, CH$_2$–O), 3.63 (t, J = 6.3 Hz, 4H, N–CH$_2$), 2.98 (s, 1H, C≡CH), 2.04 (s, 6H, 2 × CH$_3$).

4-[*N*,*N*-Bis(2-hydroxyethyl)amino]phenylacetylene (7d). Compound **7c** (0.5 g, 2 mmol) was dissolved in methanol (10 mL), sodium carbonate (0.43 g, 4 mmol) was added, and the reaction mixture was stirred at room temperature for 24 h. The solid part was collected by filtration and washed with methanol (25 mL), and the solvent was evaporated to obtain the product in 95% yield (0.4 g) as a yellow solid. Mp 107−108 °C (lit.[57] mp 107−108 °C); ^{1}H NMR (300 MHz, CDCl$_3$) δ 7.36 (d, J = 9.1 Hz, 2H, H$_{ar}$), 6.62 (d, J = 9.1 Hz, 2H, H$_{ar}$), 3.88 (t, J = 5.1 Hz, 4H, CH$_2$–O), 3.62 (t, J = 5.1 Hz, 4H, N–CH$_2$), 2.98 (s, 1H, C≡CH), 2.92 (br s, 2H, OH).

4-(*N*,*N*-Diphenylamino)phenylacetylene (7b). Method A: Potassium *tert*-butoxide (2.3 g, 20 mmol) was dissolved in dry THF (40 mL) under nitrogen. A solution was cooled to −78 °C and was stirred for 20 min at this temperature. To the cooled and stirred solution was added (bromomethyl)tri-phenylphosphonium bromide (3.45 g, 7.9 mmol) in small portions under an atmosphere of nitrogen. The reaction mixture was stirred at −78 to −65 °C for 2 h, then cooled to −78 °C and a solution of **10b** (1.35 g, 4.94 mmol) in THF (10 mL) was added dropwise. Consequently, the mixture was stirred at −78 °C for 1 h, and then at room temperature for 48 h. After this time, the reaction mixture was poured into an aqueous solution of NH$_4$Cl, acidified with a 3 M solution of hydrochloric acid, and extracted with ethyl acetate (3 × 25 mL). The crude product was purified by column chromatography on silica gel (eluent hexanes/chloroform = 4:1) to yield the title compound (0.8 g, 60%) as a yellow solid.

R_f 0.48 (SiO$_2$, hexanes/CHCl$_3$ = 4:1); mp 80−82 °C (lit.[31] mp 80−82 °C); ^{1}H NMR (300 MHz, CDCl$_3$) δ 7.33 (d, J = 8.8 Hz, 2H, H$_{ar}$), 7.29−7.24 (m, 4H, H$_{ar}$), 7.11−7.03 (m, 6H, H$_{ar}$), 6.96 (d, J = 8.8 Hz, 2H, H$_{ar}$), 3.02 (s, 1H, −C≡CH).

(Bromomethyl)triphenylphosphonium Bromide. Triphenyl-phosphine (10.0 g, 38 mmol) was dissolved in toluene (80 mL) and dibromomethane (5.5 mL, 76 mmol) was added. The reaction mixture was refluxed for 24 h, while a white precipitate was formed. The precipitate was collected by filtration, and a solution was refluxed for a further 24 h. The next part of the precipitate was filtered out, providing an overall yield of 9.9 g (60%) of (bromomethyl)triphenylphosphonium bromide. Mp 238−240 °C (lit.[58] mp 238−240 °C); ^{1}H NMR (300 MHz, CDCl$_3$) δ 7.90−7.97 (m, 6H, H$_{ar}$), 7.65−7.82 (m, 9H, H$_{ar}$), 5.84 (d, J = 5.8 Hz, 2H, −CH$_2$−Br).

Method B: To a solution of **10b** (6.6 g, 25 mmol) and PPh$_3$ (13.4 g, 51 mmol) in dry CH$_2$Cl$_2$ (150 mL), cooled to −10 °C, was added a solution of CBr$_4$ (9.95 g, 2.9 mL, 30 mmol) in CH$_2$Cl$_2$ (50 mL) under nitrogen. The reaction mixture was stirred at room temperature for 2 h. The solid part was collected by filtration and washed with CH$_2$Cl$_2$ and the combined organic layers were evaporated. The crude product was purified by column chromatography on silica gel (eluent CHCl$_3$/hexanes = 10:1) to yield 7.3 g (68%) of [4-(2,2-dibromovinyl)phenyl]diphenylamine (**14**). R_f 0.59 (SiO$_2$, EtOAc/hexanes = 1:3); ^{1}H NMR (300 MHz, CDCl$_3$) δ 7.43 (d, J = 8.7 Hz, 2H, H$_{ar}$), 7.38 (s, 1H, −CH═CBr$_2$), 7.29−7.24 (m, 4H, H$_{ar}$), 7.12−7.03 (m, 6H, H$_{ar}$), 7.00 (d, J = 8.7 Hz, 2H, H$_{ar}$).

To a solution of dibromo compound **14** (5.0 g, 11.6 mmol) in dry THF (30 mL), cooled to −78 °C, was added a 1.6 M solution of *n*-BuLi in hexanes (18 mL, 29 mmol) dropwise with stirring under an atmosphere of nitrogen. Stirring was continued at −78 °C for a further 1 h, and then the temperature was allowed to increase to room temperature. After dilution with a 20% aqueous solution of NH$_4$Cl (30 mL) and extraction with ether (3 × 30 mL), the combined organic layers were washed with a 10% aqueous solution of NH$_4$Cl (25 mL) and brine (25 mL) and dried over anhydrous Na$_2$SO$_4$, then solvents were evaporated. The title compound **7b** was obtained by column chromatography on silica gel (eluent hexanes/chloroform = 4:1) in 45% (1.4 g) yield.

General Procedure for the Preparation of Target Compounds 1a−d (Sonogashira Coupling). To a mixture of 2,6-diiodobenzothiazole **5** (0.2 g, 0.52 mmol), Pd(PPh$_3$)$_2$Cl$_2$ (36 mg, 0.052 mmol), and copper iodide (4 mg, 0.021 mmol) was added THF (8 mL) under nitrogen and the suspension was stirred at room temperature for 15 min. Consequently, 5 mL of triethyl-amine, freshly distilled from CaH$_2$, was added. After stirring for 30 min at room temperature, corresponding acetylene **7a−d** (1.24 mmol) dissolved in 2 mL of THF was added dropwise. The reaction mixture was stirred under nitrogen at room temperature for 24 h, the precipitate was collected by filtration and washed with THF, and solvents were evaporated. The crude products were purified by column chromatography.

2,6-Bis[4-(*N*,*N*-dimethylamino)phenylethynyl]benzothiazole (1a): chromatography on SiO$_2$, eluent CHCl$_3$/hexanes = 1:1; yield 80%; R_f 0.11 (SiO$_2$, CHCl$_3$/hexanes = 1:1); mp 242−245 °C; ^{1}H NMR (300 MHz, CDCl$_3$) δ 7.95 (d, J = 1.6 Hz,

(57) Huang, J. H.; Wen, W. H.; Sun, Y. Y.; Chou, P. T.; Fang, J. M. *J. Org. Chem.* **2005**, *70*, 5827–5832.

(58) Lawrence, N. J.; Liddle, J.; Jackson, D. *J. Chem. Soc., Perkin Trans. 1* **2002**, 2260–2267.

1H, H-7), 7.94 (d, J = 8.6 Hz, 1H, H-4), 7.59 (dd, J = 8.5 Hz, 1.6 Hz, 1H, H-5), 7.51 (d, J = 8.9 Hz, 2H, H$_{ar}$), 7.43 (d, J = 8.8 Hz, 2H, H$_{ar}$), 6.67 (dd, J = 8.8 Hz, 0.9 Hz, 4H, H$_{ar}$), 3.03 (s, 6H, 2 × CH$_3$), 3.00 (s, 6H, 2 × CH$_3$); ^{13}C NMR (75 MHz, CDCl$_3$) δ 152.2, 151.1, 150.2, 150.0, 135.4, 133.7 (2×), 132.8 (2×), 129.8, 123.7, 122.8, 121.8, 111.8 (2×), 111.6 2×), 109.7, 107.0, 99.5, 92.1, 87.1, 81.9, 40.2 (2×), 40.1 (2×). Anal. Calcd for C$_{27}$H$_{23}$N$_3$S: C 76.93, H 5.50, N 9.97. Found: C 77.14, H 5.38, N 10.10.

2,6-Bis[4-(*N,N*-diphenylamino)phenylethynyl]benzothiazole (1b): chromatography on SiO$_2$, eluent CHCl$_3$/hexanes = 2:3; yield 74%; R_f 0.24 (SiO$_2$, CHCl$_3$/hexanes = 2:3); mp 211–213 °C; ^{1}H NMR (300 MHz, CDCl$_3$) δ 7.99 (d, J = 1.6 Hz, 1H, H-7), 7.97 (d, J = 8.4 Hz, 1H, H-4), 7.61 (dd, J = 8.4 Hz, 1.6 Hz, 1H, H-5), 7.46 (d, J = 8.9 Hz, 2H, H$_{ar}$), 7.39 (d, J = 8.8 Hz, 2H, H$_{ar}$), 7.34–7.28 (m, 8H, NPh$_2$), 7.16–7.05 (m, 12H, NPh$_2$), 7.02 (d, J = 8.8 Hz, 2H, H$_{ar}$), 7.00 (d, J = 8.8 Hz, 2H, H$_{ar}$); ^{13}C NMR (75 MHz, CDCl$_3$) δ 152.4, 149.8, 149.5, 148.1, 147.1, 146.6, 135.5, 133.3, 132.6, 130.1, 129.6, 129.4, 125.6, 125.1, 124.3, 124.0, 123.6, 123.0, 122.1, 121.5, 121.0, 115.6, 112.5, 98.1, 91.3, 88.2, 82.3. Anal. Calcd for C$_{47}$H$_{31}$N$_3$S: C 84.28, H 4.66, N 6.27. Found: C 84.56, H 4.49, N 6.30.

2,6-Bis{4-[*N,N*-bis(2-acetoxyethyl)amino]phenylethynyl}benzothiazole (1c): chromatography on Al$_2$O$_3$ (B II., neutral), eluent hexanes/EtOAc = 1:1; yield 57%; R_f 0.5 (Al$_2$O$_3$, hexanes/EtOAc = 1:1); mp 183–185 °C; ^{1}H NMR (300 MHz, CDCl$_3$) δ 7.97 (d, J = 1.1 Hz, 1H, H-7), 7.96 (d, J = 8.5 Hz, 1H, H-4), 7.60 (dd, J = 8.5, 1.6 Hz, 1H, H-5), 7.51 (d, J = 8.8 Hz, 2H, H$_{ar}$), 7.20 (d, J = 9.0 Hz, 2H, H$_{ar}$), 6.75 (d, J = 9.0 Hz, 2H, H$_{ar}$), 6.73 (d, J = 9.0 Hz, 2H, H$_{ar}$), 4.26 (t, J = 8.5 Hz, 8H, CH$_2$–O), 3.67–3.64 (m, 8H, N–CH$_2$), 2.06 (s, 12H, 4 × CH$_3$); ^{13}C NMR (75 MHz, CDCl$_3$) δ 170.92 (2×), 170.88 (2×), 152.3, 149.9, 148.4, 147.3, 135.4, 134.0 (2×), 133.1 (2×), 129.9, 123.8, 122.9, 121.7, 111.7 (4×), 110.7, 108.2, 98.7, 91.7, 87.4, 82.0, 61.2 (2×), 61.1 (2×), 49.52 (2×), 49.48 (2×), 20.89 (2×), 20.87 (2×). Anal. Calcd for C$_{39}$H$_{39}$N$_3$O$_8$S: C 65.99, H 5.54, N 5.92. Found: C 66.24, H 5.41, N 5.88.

2,6-Bis{4-[*N,N*-bis(2-hydroxyethyl)amino]phenylethynyl}benzothiazole (1d): chromatography on Al$_2$O$_3$ (B II., neutral), eluent CHCl$_3$/MeOH = 9:1; yield 66%; R_f 0.3 (Al$_2$O$_3$, CHCl$_3$/MeOH = 9:1); mp 300 °C dec; ^{1}H NMR (300 MHz, DMSO) δ 8.30 (d, J = 1.6 Hz, 1H, H-7), 7.96 (d, J = 8.5 Hz, 1H, H-4), 7.62 (dd, J = 8.5, 1.6 Hz, 1H, H-5), 7.47 (d, J = 8.8 Hz, 2H, H$_{ar}$), 7.35 (d, J = 8.8 Hz, 2H, H$_{ar}$), 6.78 (d, J = 9.1 Hz, 2H, H$_{ar}$), 6.72 (d, J = 8.8 Hz, 2H, H$_{ar}$), 4.83–4.77 (m, 4H, OH), 3.58–3.46 (m, 16H, 4 × CH$_2$–O, 4 × N–CH$_2$); ^{13}C NMR (75 MHz, DMSO) δ 151.9, 149.6, 149.3, 148,3, 135.1, 133.6 (2×), 132.7 (2×), 129.7, 124.3, 122.7, 121.0, 111.6 (4×), 111.3, 107.3, 104.4, 92.6, 86.9, 81.8, 58.0 (4×), 53.1 (4×). Anal. Calcd for C$_{31}$H$_{31}$N$_3$O$_4$S: C 68.74, H 5.77, N 7.76. Found: C 68.93, H 5.50, N 7.90.

General Procedure for the Preparation of Compounds 9a and 9b (Suzuki Coupling). To a solution of corresponding acetylene (7a or 7b, 1.0 mmol) in THF (4 mL) was added catecholborane (0.13 mL, 1.2 mmol) under an atmosphere of nitrogen, then the solution was heated to reflux. After 1.5 h an additional amount of catecholborane (0.1 mL, 1.0 mmol) was added and heating was continued for a further 2 h. After cooling to rt, a solution of 6-iodo-2-methylbenzothiazole (8) (0.17 g, 0.625 mmol) and Pd(PPh$_3$)$_4$ (260 mg, 0.23 mmol) in THF (5 mL) was added dropwise, and the reaction mixture was stirred at room temperature for 30 min. Consequently,

20% aqueous Na$_2$CO$_3$ (1 mL) was added slowly and the mixture was heated to reflux for 20 h. After this time, the reaction mixture was cooled, quenched with water (10 mL), and extracted with ethyl acetate (3 × 30 mL). The combined organic extracts were washed with water and brine and dried over anhydrous Na$_2$SO$_4$. The resulting products were purified by column chromatography on silica gel (eluent EtOAc/hexanes = 1:3).

(*E*)-6-[4-(*N,N*-Dimethylamino)phenylethenyl]-2-methylbenzothiazole (9a): yield 78%; R_f 0.53 (SiO$_2$, EtOAc/hexanes = 1:2); mp 187–189 °C; ^{1}H NMR (300 MHz, CDCl$_3$) δ 7.88 (d, J = 1.6 Hz, 1H, H-7), 7.87 (d, J = 8.4 Hz, 1H, H-4), 7.58 (dd, J = 8.6, 1.6 Hz, 1H, H-5), 7.43 (d, J = 8.7 Hz, 2H, H$_{ar}$), 7.09 (d, J = 16.3 Hz, 1H, –CH=), 6.98 (d, J = 16.3 Hz, 1H, –CH=), 6.72 (d, J = 8.8 Hz, 2H, H$_{ar}$), 2.99 (s, 6H, NMe$_2$), 2.82 (s, 3H, CH$_3$); ^{13}C NMR (75 MHz, CDCl$_3$) δ 166.5, 152.3, 150.0, 136.4, 135.3, 129.3, 127.6, 124.3, 123.8, 122.2, 118.5, 112.6, 40.6, 20.2. Anal. Calcd for C$_{18}$H$_{18}$N$_2$S: C 73.43, H 6.16, N 9.51. Found: C 73.51, H 6.10, N 9.67.

(*E*)-6-[4-(*N,N*-Diphenylamino)phenylethenyl]-2-methylbenzothiazole (9b): yield 90%; R_f 0.29 (SiO$_2$, EtOAc/hexanes = 1:3); mp 161–164 °C; ^{1}H NMR (300 MHz, CDCl$_3$) δ 7.90 (d, J = 1.6 Hz, 1H, H-7), 7.89 (d, J = 8.4 Hz, 1H, H-4), 7.60 (dd, J = 8.5, 1.6 Hz, 1H, H-5), 7.39 (d, J = 8.6 Hz, 2H, H$_{ar}$), 7.29–7.23 (m, 4H, H$_{ar}$), 7.13–7.00 (m, 10H, H$_{ar}$, –CH=CH–), 2.83 (s, 3H, CH$_3$); ^{13}C NMR (75 MHz, CDCl$_3$) δ 167.9, 150.6, 147.7, 147.4, 135.5, 135.4, 131.0, 129.3, 129.2, 127.4, 125.9, 125.0, 124.6, 123.3, 123.2, 121.8, 118.9, 19.7. Anal. Calcd for C$_{28}$H$_{22}$N$_2$S: C 80.35, H 5.30, N 6.69. Found: C 80.52, H 5.21, N 6.85.

General Procedure for the Preparation of Target Compounds 2a and 2b (Aldol-Type Condensations). To a solution of intermediate 9a or 9b (0.4 mmol) in DMSO (5 mL) was added the corresponding 4-substituted benzaldehyde (10a or 10b, 0.4 mmol) and a 50% aqueous solution of KOH (1 mL) as a base catalyst. The reaction mixture was stirred at room temperature for 4 h. After this time, the precipitate was collected by filtration, washed with cold methanol, and dried to give the title compounds in 65% (2a) and 55% (2b) yields.

(*E,E*)-2,6-Bis[4-(*N,N*-dimethylamino)phenylethenyl]benzothiazole (2a): R_f 0.34 (SiO$_2$, EtOAc/hexanes = 1:2); mp 270–274 °C; ^{1}H NMR (300 MHz, CDCl$_3$) δ 7.89 (d, J = 1.4 Hz, 1H, H-7), 7.86 (d, J = 8.8 Hz, 1H, H-4), 7.58 (dd, J = 8.5, 1.6 Hz, 1H, H-5), 7.48 (d, J = 8.8 Hz, 2H, H$_{ar}$), 7.44 (d, J = 8.5 Hz, 2H, H$_{ar}$), 7.42 (d, J = 16.2 Hz, 1H, –CH=), 7.19 (d, J = 16.2 Hz, 1H, –CH=), 7.11 (d, J = 16.2 Hz, 1H, –CH=), 6.99 (d, J = 16.2 Hz, 1H, –CH=), 6.73 (d, J = 8.8 Hz, 2H, H$_{ar}$), 6.72 (d, J = 8.8 Hz, 2H, H$_{ar}$), 3.03 (s, 6H, NMe$_2$), 3.00 (s, 6H, NMe$_2$); ^{13}C NMR (75 MHz, CDCl$_3$) δ 167.7, 153.1, 151.2, 150.2, 137.9, 135.4, 134.9, 129.2, 128.9, 127.6, 125.6, 124.5, 123.8, 123.4, 122.3, 118.3, 117.4, 112.4, 112.1, 40.5, 40.2. Anal. Calcd for C$_{27}$H$_{27}$N$_3$S: C 76.20, H 6.39, N 9.87. Found: C 76.33, H 6.16, N 9.91.

(*E,E*)-2,6-Bis[4-(*N,N*-diphenylamino)phenylethenyl]benzothiazole (2b): R_f 0.58 (SiO$_2$, EtOAc/hexanes = 1:2), mp 188–190 °C; ^{1}H NMR (300 MHz, CDCl$_3$) δ 7.92 (d, J = 1.5 Hz, 1H, H-7), 7.90 (d, J = 8.6 Hz, 1H, H-4), 7.58 (dd, J = 8.6, 1.6 Hz, 1H, H-5), 7.46–7.39 (m, 5H, H$_{ar}$, –CH=CH–), 7.32–7.24 (m, 4H, H$_{ar}$), 7.16 – 7.02 (m, 23H, H$_{ar}$, –CH=CH–); ^{13}C NMR (75 MHz, CDCl$_3$) δ 167.4, 153.2, 149.1, 147.5, 147.4, 147.0, 137.2, 135.1, 135.0, 131.2, 129.4, 129.3, 128.70, 128.66, 128.4, 127.4, 126.2, 125.2, 124.9, 124.6,

123.8, 123.4, 123.1, 122.6, 122.2, 119.8, 118.9. Anal. Calcd for $C_{47}H_{35}N_3S$: C 83.77, H 5.24, N 6.24. Found: C 83.86, H 5.07, N 6.38.

II. Two-Photon and Time-Resolved Fluorescence Measurements. The two-photon absorption cross sections, δ_{TPA}, of the benzothiazole dyes were determined via Two-Photon Excited Fluorescence (TPEF).[12,22,59] The excitation source was a mode-locked Ti:Sapphire laser operating in the femtosecond time domain (pulse duration 80 fs and repetition rate 80 MHz). The laser beam was tunable from 750 to 850 nm. The pulse duration, excitation power, and pulse spectrum were continuously monitored during the experiment. Before exciting the samples, the laser beam was expanded through a 5-fold expanding telescope to obtain a top-hat excitation beam profile and uniformly illuminate the back aperture of the objective lens (NA = 0.32) that was used for the excitation of the samples. The TPA-induced fluorescence was collected backward by the same lens and was separated from the excitation beam by using a dichroic mirror and a series of short-pass filters. Finally, it was detected by a photomultiplier connected to photon counting electronics. The TPA fluorescence intensity was measured as a function of the excitation power every 10 nm within the wavelength range of the excitation laser. In all cases, the calculations of δ_{TPA} were made within the power regime, where the fluorescence was proportional to the square of the excitation power, in order to ensure that effects like saturation, excited state absorption, etc. are negligible and the observed fluorescence was only due to two-photon absorption. The samples were 10^{-4} M solutions of the benzothiazole dyes in THF placed in $1 \times 1 \times 3$ cm^3 quartz cuvettes. A reference experiment was also performed in which a neat THF sample was used to measure the background signal. This signal was afterward subtracted from the TPA fluorescence signal of the dyes. The values of δ_{TPA} were determined by using rhodamine B (10^{-4} M in methanol) as a reference, which has a well-known TPA spectrum. For the calculation of δ_{TPA}, it was assumed that the fluorescence quantum yield is the same under two-photon or one-photon excitation following the analysis of Xu et al.[59]

Time-resolved fluorescence dynamics was studied in THF solutions using a femtosecond fluorescence upconversion technique. The technique provides 160 fs temporal resolution and has been described in detail previously.[60] Briefly, the same Ti:Sapphire mode locked laser emitting 80 fs pulses at 800 nm was used as a light source. The second harmonic of the femtosecond laser, at 400 nm, with average power of less than 2 mW, was used for the excitation of the samples which were contained in a rotating cell with 0.8 mm path length. The remaining fundamental beam, at 800 nm, passed through a delay line with 0.01 μm resolution and was used as the gate beam. The fluorescence of the samples was collected and mixed together with the delayed gate beam into a 0.5 mm BBO crystal (type I mixing) generating an upconversion beam. This beam passed through a monochromator and was detected through a photomultiplier as a function of the temporal delay between the gate beam and the fluorescence. The fluorescence decays of the samples

were detected at the fluorescence maximum wavelength of each sample under magic angle conditions.

III. Computational Details. The ground-state structures of all molecules under investigation (**1**−**4**) were fully optimized at the B3LYP[61] level of theory employing TZVP[62] basis set and were characterized as the true minima on the harmonic potential energy hypersurfaces. The long alkyl chains in **3** were replaced by the methyl groups for simplification of calculation. To obtain the fluorescence energies (E_{em}), the first excited-state geometries were fully optimized by using the time-dependent DFT method, employing the same exchange-correlation functional and basis set as was used in the ground-state structure optimization. All these calculations were carried out with the Turbomole program.[63]

The time-dependent DFT method with the 6-31G(d) basis set and the B3LYP or the Coulomb-attenuated CAM-B3LYP[64] exchange-correlation functional, as implemented in the Gaussian 09 program package,[65] was applied to get excitation energies (E_{max}), transition dipole moments (μ_{0n}), and adiabatic dipole moment changes ($\Delta\mu_{0n}$) between the ground state and the n-th excited state. The atomic charges in the ground state and the first two excited states were calculated by the natural population analysis (NPA),[66] using the built-in NBO-3.1 subroutines of the Gaussian 09 program. The excited-to-excited transition dipole moments μ_{12} were obtained from the double-residue of the quadratic response function. The latter calculations were carried out with the Dalton program.[67] Solvent effects were simulated by employing a polarizable continuum model (PCM).[42,68]

The TPA cross sections δ_{TPA} were evaluated by calculating the two-photon transition moment matrix elements $S_{\alpha\beta}$ in the Dalton program. The matrix elements $S_{\alpha\beta}$ for the two-photon resonant absorption of identical energy can be identified from the sum-overstates (SOS) formula as:

$$S_{\alpha\beta} = \sum_n \left[\frac{\langle 0|\mu_\alpha|n\rangle\langle n|\mu_\beta|f\rangle}{\omega_n - \frac{\omega_f}{2}} + \frac{\langle 0|\mu_\beta|n\rangle\langle n|\mu_\alpha|f\rangle}{\omega_n - \frac{\omega_f}{2}} \right]$$
$$(\alpha, \beta = x, y, z)$$

where ω_n represents the excitation energy from the ground state $|0\rangle$ to the excited state $|n\rangle$, $\omega_f/2$ corresponds to half of the excitation energy associated with the transition from the ground to the final excited state $|f\rangle$, and μ_α and μ_β are the Cartesian components of the electronic dipole moment operator. The computation of $S_{\alpha\beta}$ is a demanding task, because it formally involves explicit summation over all excited states of the molecule. This summation was, however,

(59) Xu, C.; Webb, W. W. *J. Opt. Soc. Am. B* **1996**, *13*, 481–491.

(60) Fakis, M.; Polyzos, I.; Tsigaridas, G.; Giannetas, V.; Persephonis, P. *Chem. Phys. Lett.* **2004**, *394*, 372–376. Fakis, M.; Anestopoulos, D.; Giannetas, V.; Persephonis, P. *J. Phys. Chem. B* **2006**, *110*, 24897–24902.

(61) Becke, A. D. *J. Chem. Phys.* **1993**, *98*, 1372–1377. Stephens, P. J.; Devlin, F. J.; Chabalowski, C. F.; Frisch, M. J. *J. Phys. Chem.* **1994**, *98*, 11623–11627.

(62) Schafer, A.; Huber, C.; Ahlrichs, R. *J. Chem. Phys.* **1994**, *100*, 5829–5835.

(63) TURBOMOLE, a development of University of Karlsruhe and Forschungszentrum Karlsruhe GmbH, version 6.0, **2009**.

(64) Yanai, T.; Tew, D. P.; Handy, N. C. *Chem. Phys. Lett.* **2004**, *393*, 51–57.

(65) Frisch, M. J.; et al. *Gaussian 09*, revision A.01; Gaussian, Inc.: Wallingford, CT, 2009.

(66) Reed, A. E.; Curtiss, L. A.; Weinhold, F. *Chem. Rev.* **1988**, *88*, 899–926.

(67) *DALTON, a molecular electronic structure program*, Release 2.0, **2005** (see http://www.kjemi.uio.no/software/dalton/dalton.html).

(68) Tomasi, J.; Persico, M. *Chem. Rev.* **1994**, *94*, 2027–2094. Tomasi, J.; Mennucci, B.; Cammi, R. *Chem. Rev.* **2005**, *105*, 2999–3093.

avoided through the use of quadratic response theory. Within this formalism, matrix elements $S_{\alpha\beta}$ are extracted as a single residue of the appropriate quadratic response function for the dipole moment operators. This approach is described in detail in ref 69.

With the $S_{\alpha\beta}$ elements in hand, the TPA cross-section of the molecule for linearly polarized monochromatic light was calculated (in atomic units) as:

$$\delta_{\text{a.u.}} = \frac{1}{30}\sum_{\alpha,\beta}(2S_{\alpha\alpha}S_{\beta\beta}{}^* + 4S_{\alpha\beta}S_{\beta\alpha}{}^*)$$

The final expression for the TPA cross-section, which is directly comparable to experiment, was used:

$$\delta_{\text{TPA}} = \frac{(2\pi)^3\alpha a_0{}^5}{c}\frac{\omega^2}{\pi\Gamma}\delta_{\text{a.u.}}$$

Here, α is the fine structure constant, a_0 is the Bohr radius, c is the speed of light, ω is the energy of the exciting photon (in case of the TPA process, one-half of the excitation energy), and $\pi\Gamma$ is a normalization factor due to the Lorentzian line-shape broadening of the excited state ($\Gamma = 0.2\,\text{eV}$

was assumed throughout this work). The units of δ_{TPA} will become GM ($\text{cm}^4\cdot\text{s}\cdot\text{photon}^{-1}$), provided we use centimeter·gram·second units for a_0 and c, and atomic units for ω and Γ.

Supporting Information Available: General experimental methods, synthetic procedures (not covered in the article), ^{1}H and ^{13}C NMR spectra of new compounds (**1a−d**, **2a,b**, **5**, **9a,b**), optical properties of **1−4** calculated at the B3LYP/6-31G(d) level of theory, TPA cross sections computed using the PCM solvation model, NPA charge analysis of the ground state and the first two excited states, and Cartesian coordinates of the optimized ground-state structures. This material is available free of charge via the Internet at http://pubs.acs.org.

(69) Norman, P.; Ruud, K. Microscopic theory of nonlinear optics. In *Nonlinear optical properties of matter: From molecules to condensed phases*; Springer: Dordrecht, The Netherlands, 2006; Chapter 1, pp 1−49.